

1 **Conformational features and ionization states of Lys side chains in a protein**  
2 **revealed** by the stereo-array isotope labeling (SAIL) method

3

4 Mitsuhiro Takeda<sup>1,2</sup>, Yohei Miyanoiri<sup>1,3</sup>, Tsutomu Terauchi<sup>4,5</sup>,  
5 and Masatsune Kainosho<sup>1,5\*</sup>

6

7 <sup>1</sup>Structural Biology Research Center, Graduate School of Science, Nagoya University, Furo-cho,  
8 Chikusa-ku, Nagoya, 464-8602 Japan; <sup>2</sup>Department of Structural BioImaging, Faculty of Life  
9 Sciences, Kumamoto University, 5-1, Oe-honmachi, Chuo-ku, Kumamoto, 862-0973 Japan;

10 <sup>3</sup>Research Center for State-of-the-Art Functional Protein Analysis, Institute for Protein Research,  
11 Osaka University, 3-2 Yamadaoka, Suita, Osaka, 565-0871 Japan; <sup>4</sup>SAIL Technologies Co., Inc.,  
12 2008-2 Wada, Tama-city, Tokyo, 206-0001 Japan; <sup>5</sup>Graduate School of Science, Tokyo  
13 Metropolitan University, 1-1 Minami-ohsawa, Hachioji, Tokyo, 192-0397 Japan

14

15 \*Correspondence should be addressed to:

16 Masatsune Kainosho, Ph.D.

17 Graduate School of Science, Tokyo Metropolitan University, 1-1 Minami-ohsawa, Hachioji,  
18 Tokyo 192-0397, Japan

19 E.mail: [kainosho@tmu.ac.jp](mailto:kainosho@tmu.ac.jp)

20

21 Dedicated to Professor Robert Kaptein on the occasion of his 80<sup>th</sup> birthday.

## 22 Abstract

23 Although both the *hydrophobic* aliphatic chain and *hydrophilic*  $\zeta$ -amino group of the Lys side  
24 chain presumably contribute to the structures and functions of proteins, the *dual* nature of the Lys  
25 residue has not been fully investigated by NMR spectroscopy, due to the lack of appropriate  
26 methods to acquire comprehensive information on its long consecutive methylene chain. We  
27 describe herein a robust strategy to address the current situation, using various isotope-aided NMR  
28 technologies. The feasibility of our approach is demonstrated for the  $\Delta$ +PHS/V66K variant of  
29 *Staphylococcal* nuclease (SNase), which contains 21 Lys residues, including the engineered Lys-  
30 66 with an unusually low  $pK_a$  of  $\sim 5.6$ . All of the NMR signals for the 21 Lys residues were  
31 sequentially and stereo-specifically assigned by using the stereo-array isotope labeled Lys (SAIL-  
32 Lys), [U- $^{13}\text{C}$ ,  $^{15}\text{N}$ ;  $\beta_2, \gamma_2, \delta_2, \epsilon_3$ -D $_4$ ]-Lys. The complete set of the assigned  $^1\text{H}$ -,  $^{13}\text{C}$ -,  $^{15}\text{N}$ -NMR signals  
33 for the Lys sidechain moieties affords various structural information, for example, relative  
34 orientations of the Lys sidechains against nearby aromatic rings. The  $^{13}\text{C}^\epsilon$  and  $^{15}\text{N}^\zeta$  chemical shifts  
35 of the SNase variant selectively labeled with either [ $\epsilon$ - $^{13}\text{C}$ ;  $\epsilon, \epsilon$ -D $_2$ ]-Lys or SAIL-Lys dissolved in  
36 H $_2\text{O}$  and D $_2\text{O}$  showed that deuterium induced shifts for Lys-66 were substantially different from  
37 the rest of the Lys residues. Namely, the deuterium-induced shifts of the  $^{13}\text{C}^\epsilon$  and  $^{15}\text{N}^\zeta$  signals  
38 depend on the ionization states of the  $\zeta$ -amino group; i.e., -0.32 ppm for  $\Delta\delta^{13}\text{C}^\epsilon$  [ $\text{N}^\zeta\text{D}_3^+ - \text{N}^\zeta\text{H}_3^+$ ] vs.  
39 -0.21 ppm for  $\Delta\delta^{13}\text{C}^\epsilon$  [ $\text{N}^\zeta\text{D}_2 - \text{N}^\zeta\text{H}_2$ ], and -1.1 ppm for  $\Delta\delta^{15}\text{N}^\zeta$  [ $\text{N}^\zeta\text{D}_3^+ - \text{N}^\zeta\text{H}_3^+$ ] vs. -1.8 ppm for  
40  $\Delta\delta^{15}\text{N}^\zeta$  [ $\text{N}^\zeta\text{D}_2 - \text{N}^\zeta\text{H}_2$ ]. Since the 1D- $^{13}\text{C}$  NMR spectrum of a protein selectively labeled with [ $\epsilon$ - $^{13}\text{C}$ ;  
41  $\epsilon, \epsilon$ -D $_2$ ]-Lys shows extremely narrow ( $> 2$  Hz) and well-dispersed  $^{13}\text{C}$  signals, the deuterium-  
42 induced isotope shifts difference of 0.11 ppm for the protonated and deprotonated  $\zeta$ -amino groups,  
43 which corresponds to 16.5 Hz at a field strength of 14 tesla (150 MHz for  $^{13}\text{C}$ ), will be a versatile  
44 index for searching the Lys residues having deprotonated  $\zeta$ -amino groups at physiological pHs in  
45 larger proteins containing numerous Lys residues.

46

47

## 48 **1 Introduction**

49 Detailed studies on the structures and dynamics of the Lys residues in a protein have been severely  
50 hampered by the difficulty in gathering comprehensive NMR information on their side chain  
51 moieties. It is especially challenging to establish *unambiguous* stereo-specific assignments for the  
52 prochiral protons in the four consecutive methylene chain, which is the longest aliphatic chain  
53 among the 20 common amino acids. Given the lack of generally applicable strategies to overcome  
54 this obstacle, only a few systematic  $^1\text{H}$ -NMR studies using stereospecifically assigned have probed  
55 the structural aspects of the Lys residues. The ionization states of the Lys  $\zeta$ -amino groups also  
56 provide important information, as they are often involved in specific intra- and/or intermolecular  
57 molecular recognition processes, and thus play vital roles in protein functions. Therefore, the side  
58 chain moieties of Lys residues are considered to contribute to maintaining the structure and  
59 biological functions of a protein by these two elements: the *hydrophobic* methylene chain and the  
60 *hydrophilic*  $\zeta$ -amino group. To investigate the *dual* nature of the Lys side chain, we have applied  
61 various isotope-aided NMR technologies, including the stereo-array isotope labeling (SAIL)  
62 method (Kainosho et al., 2006).

63 The Lys  $\zeta$ -amino groups, which usually have  $\text{pK}_a$  values around 10.5, are protonated ( $\text{NH}_3^+$ )  
64 at around neutral pH. However, certain proteins have Lys residues with deprotonated  $\zeta$ -amino  
65 groups even at neutral or acidic pH (Harris and Turner, 2002). In such cases, the  $\text{pK}_a$  values of the  
66 Lys  $\zeta$ -amino groups are substantially lowered due to their particular local environments. Since the  
67 Lys  $\zeta$ - $\text{NH}_2$  groups are endowed with significantly different physical chemical properties, as  
68 compared to the  $\zeta$ - $\text{NH}_3^+$ , they can perform specific functions such as Schiff base formation through  
69 nucleophilic attacks on various substrates (Highbarger et al., 1996; Barbas et al., 1997). Although  
70 the ionization states of Lys  $\zeta$ -amino groups in a protein have been characterized by X-ray  
71 crystallography, they may not always be identical to those in solution. The  $\text{NH}_3^+$  and  $\text{NH}_2$  states  
72 of Lys residues in solution could also be identified by the cross peak patterns in the  $^1\text{H}$ - $^{15}\text{N}$   
73 correlation NMR spectra, if the hydrogen exchange rates are sufficiently slow, or by the  $^{15}\text{N}^\zeta$  and/or  
74  $^1\text{H}^\zeta$  chemical shifts (Poon et al., 2006; Iwahara et al., 2007; Takayama et al., 2008). Under  
75 physiological conditions, however, the observations of  $^1\text{H}$ - $^{15}\text{N}$  cross peaks are often hampered due

76 to the rapid hydrogen exchange rates of the Lys  $\zeta$ -amino groups (Liepinsh et al., 1992; Liepinsh  
77 and Otting, 1996; Otting and Wüthrich, 1989; Otting et al., 1991; Segawa et al., 2008). The  
78 ionization states can also be identified by the pH titration profiles for the  $^{13}\text{C}^\epsilon$  and  $^{15}\text{N}^\zeta$  signals of  
79 individual Lys residues (Kesvatera et al., 1996; Damblon et al., 1996; Farmer and Venters, 1996;  
80 Poon et al., 2006; Gao et al., 2006; André et al., 2007). Unfortunately, long-term experiments such  
81 as pH titration are hampered by the stability and solubility issues of a protein over the wide pH  
82 range. Therefore, straightforward and robust alternative methods to identify Lys residues with  
83 distinct ionization states for the  $\zeta$ -amino groups are highly desired.

84 We used a variant of *Staphylococcal* nuclease,  $\Delta$ +PHS/V66K SNase (denoted as the SNase  
85 variant, hereafter), as the model protein (Stites et al., 1991). This variant was engineered to add  
86 the following three features to the wild-type SNase: (i) introduction of three stabilizing mutations,  
87 P117G, H124L and S128A (*PHS*); (ii) deletion of amino acids 44-49 and introduction of two  
88 mutations, G50F and V51N ( $\Delta$ ); and (iii) substitution of Val66 with Lys (*V66K*). With these three  
89 modifications, the  $\Delta$ +*PHS/V66K* SNase variant becomes thermally stable, even with the  $\zeta$ -amino  
90 group of Lys-66 entrapped within the hydrophobic cavity originally occupied by the Val-66 side  
91 chain in the wild-type SNase. As a result, the  $\zeta$ -amino group of Lys-66 in the SNase variant exhibits  
92 an unusually low  $\text{pK}_a$  value of 5.7 (García-Moreno et al., 1997; Fitch et al., 2002).

93 Although the SNase variant contains 21 Lys residues (Fig. A1), including the engineered Lys-  
94 66, the  $^{13}\text{C}$ ,  $^1\text{H}$  and  $^{15}\text{N}$  NMR signals for the Lys side chains were unambiguously observed and  
95 assigned by using the SNase variant selectively labeled with SAIL-Lys; i.e., [ $^{13}\text{C}$ ,  $^{15}\text{N}$ ;  
96  $\beta_2, \gamma_2, \delta_2, \epsilon_3$ -D<sub>4</sub>]-Lys (Kainosho et al., 2006; Terauchi et al., 2011). In this article, we examine some  
97 of the structural features inferred from the comprehensive chemical shift data and the deuterium-  
98 induced isotope shifts on the  $^{13}\text{C}^\epsilon$  and  $^{15}\text{N}^\zeta$  of the Lys residues in the SNase variant, and show that  
99 the side chain NMR signals can serve as powerful probes to investigate the *dual* nature of a Lys  
100 side chain in a protein.

## 101 **2 Material and methods**

### 102 **2.1 Sample preparation**

103 The  $\Delta$ +PHS/V66K SNase variants selectively labeled with either L-[U- $^{13}\text{C}$ , $^{15}\text{N}$ ]-Lys, L-[U-  
104  $^{13}\text{C}$ , $^{15}\text{N}$ ;  $\beta_2,\gamma_2,\delta_2,\epsilon_3\text{-D}_4$ ]-Lys (SAIL-Lys), or L- $[\epsilon\text{-}^{13}\text{C};\epsilon,\epsilon\text{-D}_2]$ -Lys, which were synthesized in house,  
105 were prepared using the *E. coli* BL21 (DE3) strain transformed with a pET3 vector (Novagen),  
106 encoding the  $\Delta$ +PHS/V66K SNase gene fused with an N-terminal His-tag. The transformed *E. coli*  
107 cells were cultured at 37 °C in 500 mL of M9 medium, containing anhydrous  $\text{Na}_2\text{HPO}_4$  (3.4 g/L),  
108 anhydrous  $\text{KH}_2\text{PO}_4$  (0.5 g/L),  $\text{NaCl}$  (0.25 g/L), D-glucose (5 g/L),  $\text{NH}_4\text{Cl}$  (0.5 g/L), thiamine (0.5  
109 mg/L),  $\text{FeCl}_3$  (0.03 mM),  $\text{MnCl}_2$  (0.05 mM),  $\text{CaCl}_2$  (0.1 mM), and  $\text{MgSO}_4$  (1 mM), with 10 mg/L  
110 of the mono-hydrochloride salts of either [U- $^{13}\text{C}$ , $^{15}\text{N}$ ]-Lys, SAIL-Lys, or  $[\epsilon\text{-}^{13}\text{C};\epsilon,\epsilon\text{-D}_2]$ -Lys. Each  
111 culture was maintained at 37 °C. An additional 20 mg/L of each isotope-labeled Lys was  
112 supplemented when the  $\text{OD}_{600}$  reached 0.5, and then protein expression was induced by adding  
113 isopropyl- $\beta$ -D-thiogalactopyranoside (IPTG) to a final concentration of 0.4 mM. At 4-5 h after the  
114 induction, the cells were collected by centrifugation and the SNase variant proteins were purified  
115 on a Ni-NTA column according to the standard protocol. The enrichment levels for Lys were ~70%,  
116 as measured by mass spectrometry. The purified proteins were dissolved in 20 mM sodium  
117 phosphate buffers containing 100 mM KCl (pH 8.0), prepared with either  $\text{H}_2\text{O}$ ,  $\text{D}_2\text{O}$  or  $\text{H}_2\text{O}:\text{D}_2\text{O}$   
118 (1:1).

## 119 2.2 NMR spectroscopy

120 The 600 MHz 2D  $^1\text{H}$ - $^{13}\text{C}$  constant-time HSQC spectra of the SNase variant, selectively  
121 labeled with either [U- $^{13}\text{C}$ , $^{15}\text{N}$ ]-Lys or SAIL-Lys, were measured in  $\text{D}_2\text{O}$  at 30 °C on a Bruker  
122 Avance spectrometer equipped with a TXI cryogenic probe. For the latter sample, additional  
123 deuterium decoupling was applied during the  $t_1$  period. The data sizes and spectral widths were  
124 1,024 ( $t_1$ )  $\times$  2,048 ( $t_2$ ) points and 12,000 Hz ( $\omega_1$ ,  $^{13}\text{C}$ )  $\times$  8,700 Hz ( $\omega_2$ ,  $^1\text{H}$ ), respectively. Each set  
125 of 32 scans/FID with a 1.5 s repetition time was collected, using the  $^{13}\text{C}$  carrier frequency at 38  
126 ppm. The 600 MHz 3D HCCH-TOCSY spectrum was measured in  $\text{D}_2\text{O}$  at 30 °C for the SNase  
127 variant labeled with SAIL-Lys (Clore et al., 1990; Cavanagh et al., 2007). The data size and  
128 spectral width were 1,024 ( $t_1$ )  $\times$  32 ( $t_2$ )  $\times$  2,048 ( $t_3$ ) points and 6,000 Hz ( $\omega_1$ ,  $^1\text{H}$ ) Hz  $\times$  9,100 Hz  
129 ( $\omega_2$ ,  $^{13}\text{C}$ )  $\times$  9,000 Hz ( $\omega_3$ ,  $^1\text{H}$ ), respectively. Each set of 16 scans/FID with a 1.5 s repetition time  
130 was collected, using the  $^{13}\text{C}$  carrier frequency at 40 ppm.

131 The Lys  $\zeta$ - $^{15}\text{N}$  signals of the SAIL-Lys labeled SNase variant dissolved in  $\text{D}_2\text{O}$  at 30 °C were

132 assigned using the HECENZ pulse sequence, utilizing the out-and-back magnetization transfer  
133 from  $^1\text{H}^{\epsilon 2}$  to  $^{15}\text{N}^{\zeta}$  via  $^{13}\text{C}^{\epsilon}$ . The correlations between the  $^1\text{H}^{\epsilon 2}$  and  $^{15}\text{N}^{\zeta}$  signals for most of the 21  
134 Lys residues were firmly established by the pulse sequence, which was basically the same as the  
135 H2CN pulse sequence developed by Andre et al. (Andre et al., 2007). The data size and the spectral  
136 width were  $512 (t_1) \times 1024 (t_2)$  points and  $1,200 \text{ Hz } (\omega_1, ^{15}\text{N}) \text{ Hz} \times 9,600 \text{ Hz } (\omega_2, ^1\text{H})$ , respectively,  
137 and deuterium decoupling was applied during the  $t_1$  period. The carrier frequencies were 38 ppm  
138 and 28 ppm for  $^{13}\text{C}$  and  $^{15}\text{N}$ , respectively, and 128 scans/FID with a 2 s repetition time were  
139 accumulated.

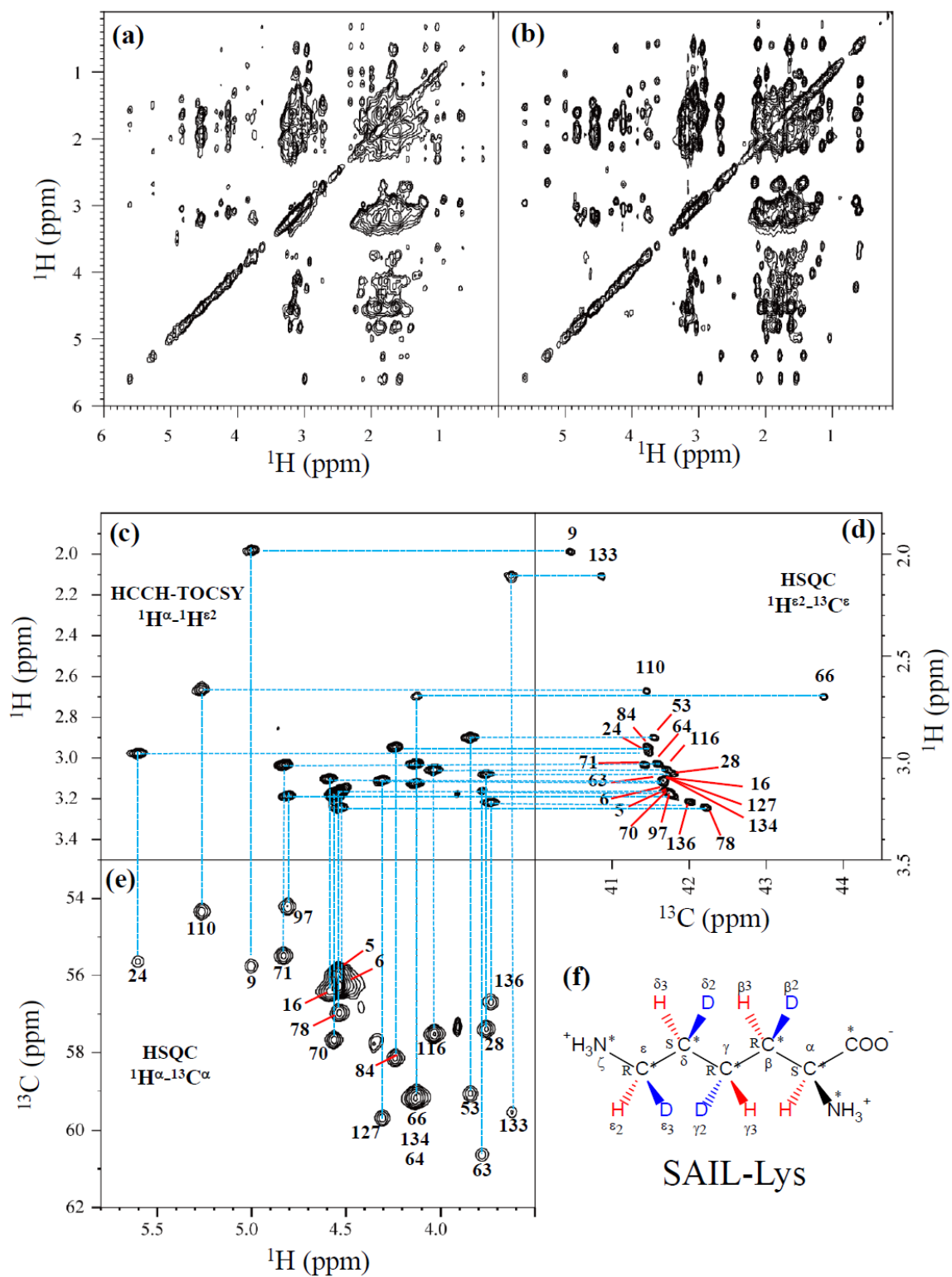
140 The 125.7 MHz 1D  $^{13}\text{C}$  NMR spectra of the SNase variant proteins selectively labeled with  
141 either  $[\text{U-}^{13}\text{C}, ^{15}\text{N}]$ -Lys or  $[\epsilon\text{-}^{13}\text{C}; \epsilon, \epsilon\text{-D}_2]$ -Lys were measured in  $\text{D}_2\text{O}$ ,  $\text{H}_2\text{O}$ , and  $\text{H}_2\text{O-D}_2\text{O}$  (1:1), at  
142 25 °C on a Bruker Avance 500 spectrometer equipped with a DCH cryogenic probe under the  
143 proton and, for the latter sample, simultaneous deuterium decoupling using the WALTZ16 scheme.  
144 The spectral width and repetition time were 6,300 Hz and 5 s, respectively. In the experiment in  
145  $\text{H}_2\text{O}$  solution, a 4.1 mm o.d. Shigemi tube containing the protein solution was inserted into a 5 mm  
146 o.d. outer tube containing pure  $\text{D}_2\text{O}$  for the internal lock signal. By taking advantage of the  
147 selective deuteration on the  $\epsilon\text{-}^{13}\text{C}$  in  $[\epsilon\text{-}^{13}\text{C}; \epsilon, \epsilon\text{-D}_2]$ -Lys (~98 atom %), the background  $^{13}\text{C}$  signals  
148 due to the naturally abundant, and therefore protonated,  $^{13}\text{C}$  nuclei were readily filtered out by  
149 using the pulse scheme shown in Fig. A2.

## 150 **3 Results and discussion**

### 151 **3.1 Complete assignment of the Lys side chain NMR signals in the SNase variant selectively** 152 **labeled with SAIL-Lys**

153 Although the chemical shifts with sequential assignments for the backbone  $^1\text{H}$ ,  $^{13}\text{C}$  and  $^{15}\text{N}$  signals  
154 of SNase are available in the BMRB (Entry #16123; Chimenti et al., 2011), we reconfirmed them  
155 by the HNCA experiment for the  $[\text{U-}^{13}\text{C}, ^{15}\text{N}]$ -SNase variant, since the solution conditions were  
156 slightly different. The complete side chain assignment for all 21 Lys residues was not trivial, even  
157 for the SNase variant residue-selectively labeled with  $[\text{U-}^{13}\text{C}, ^{15}\text{N}]$ -Lys, due to the extensive signal  
158 overlap as illustrated in the  $F1\text{-}F3$  projection of the 3D HCCH TOCSY spectrum (Fig. 1a). On the  
159 other hand, a markedly improved 3D HCCH TOCSY spectrum was obtained, under the

160 simultaneous deuterium decoupling, for the SNase variant residue-selectively labeled with SAIL-  
161 Lys (Fig. 1b), enabling us to firmly establish the full connectivity for the side chain  $^1\text{H}$ ,  $^{13}\text{C}$  and  
162  $^{15}\text{N}$  NMR signals of the 21 Lys residues. To illustrate the improved spectral quality obtained with  
163 the SAIL-Lys in lieu of  $[\text{U-}^{13}\text{C}, ^{15}\text{N}]$ -Lys, a panel obtained for the  $F1$ - $F3$  projection, along the  $^{13}\text{C}$ -  
164 axis ( $F2$ ) restricted for the chemical shift range of 40.1-45.5 ppm for the  $^{13}\text{C}^\epsilon$  signals, is shown for  
165 the  $^1\text{H}^\alpha$ - $^1\text{H}^{\epsilon 2}$  correlation signals (Fig. 1c). By taking advantage of the well-dispersed  $^1\text{H}^\alpha$ - $^1\text{H}^{\epsilon 2}$   
166 signals, the backbone  $^1\text{H}^\alpha$ - $^{13}\text{C}^\alpha$  signals (Fig. 1e) were readily correlated to the  $^1\text{H}^{\epsilon 2}$ - $^{13}\text{C}^\epsilon$  HSQC  
167 signals (Fig. 1d). Actually, all of the SAIL-Lys side chain  $^{13}\text{C}$  signals were facily and  
168 unambiguously assigned through the 3D HCCH TOCSY spectrum, yielding a complete set of the  
169 Lys side chain NMR chemical shifts, as summarized in Table 1. It should be noted that, since each  
170 one of the side chain methylene protons was *stereo-specifically* deuterated in SAIL-Lys; i.e.,  $[\text{U-}$   
171  $^{13}\text{C}, ^{15}\text{N}; \beta_2, \gamma_2, \delta_2, \epsilon_3\text{-D}_4]$ -Lys (Fig. 1f), all of the 21 Lys side chain methylene proton signals are  
172 *stereo-specifically* assigned to each of the  $\beta_3$ ,  $\gamma_3$ ,  $\delta_3$ , and  $\epsilon_2$ - $^1\text{H}$  signals, thus providing precious  
173 clues to examine the local conformations of the Lys side chains in solution.



174

175 **Figure 1: Sequential assignment of the Lys side chain signals for the SNase variant selectively**

176 **labeled with SAIL-Lys by the 3D HCCH TOCSY experiment.** Panels (a) and (b) show a  
177 comparison of the *F1-F3* projections of the 3D HCCH TOCSY spectra obtained for the SNase variant  
178 selectively labeled with either [U-<sup>13</sup>C, <sup>15</sup>N]-Lys (a) or SAIL-Lys (b). A complete side chain signal  
179 assignment was established for the SNase variant selectively labeled with SAIL-Lys by the correlation  
180 networks on the 3D HCCH TOCSY spectrum, starting from the backbone <sup>1</sup>H<sup>α</sup>, <sup>13</sup>C<sup>α</sup> signals with  
181 assignments deposited in the BMRB (Entry #16123; Chimenti et al., 2011). For example, the <sup>1</sup>H<sup>ε2</sup>-<sup>13</sup>C<sup>ε</sup>  
182 HSQC signals in panel (d) were unambiguously correlated to the backbone <sup>1</sup>H<sup>α</sup>-<sup>13</sup>C<sup>α</sup> HSQC signals in panel  
183 (e), through the <sup>1</sup>H<sup>α</sup>-<sup>1</sup>H<sup>ε2</sup> correlation signals in panel (c), which represents the *F1-F3* projection of the 3D  
184 HCCH TOCSY spectrum along the <sup>13</sup>C-axis (*F2*) restricted for the <sup>13</sup>C<sup>ε</sup> shift range of 40.1-45.5 ppm. The  
185 structure of SAIL-Lys, [U-<sup>13</sup>C, <sup>15</sup>N; β<sub>2</sub>,γ<sub>2</sub>,δ<sub>2</sub>,ε<sub>3</sub>-D<sub>4</sub>]-Lys, was shown in panel (f). **The spectrum was measured**  
186 **at 30 °C on a Bruker Avance 600 spectrometer equipped with a TXI cryogenic probe.**

~~187 <sup>15</sup>N NMR signals of the 21 Lys residues. To illustrate the improved spectral quality obtained with  
188 the SAIL-Lys in lieu of [U-<sup>13</sup>C, <sup>15</sup>N]-Lys, a panel obtained for the *F1-F3* projection, along the <sup>13</sup>C-  
189 axis (*F2*) restricted for the chemical shift range of 40.1-45.5 ppm for the <sup>13</sup>C<sup>ε</sup> signals, is shown for  
190 the <sup>1</sup>H<sup>ε</sup>-<sup>1</sup>H<sup>ε2</sup> correlation signals (Fig. 1c). By taking advantage of the well-dispersed <sup>1</sup>H<sup>ε</sup>-<sup>1</sup>H<sup>ε2</sup>  
191 signals, the backbone <sup>1</sup>H<sup>ε</sup>-<sup>13</sup>C<sup>ε</sup> signals (Fig. 1e) were readily correlated to the <sup>1</sup>H<sup>ε2</sup>-<sup>13</sup>C<sup>ε</sup> HSQC  
192 signals (Fig. 1d). Actually, all of the SAIL-Lys side chain <sup>13</sup>C signals were facilely and  
193 unambiguously assigned through the 3D HCCH TOCSY spectrum, yielding a complete set of the  
194 Lys side chain NMR chemical shifts, as summarized in Table 1. It should be noted that, since each  
195 one of the side chain methylene protons was *stereo-specifically* deuterated in SAIL-Lys; i.e., [U-  
196 <sup>13</sup>C, <sup>15</sup>N; β<sub>2</sub>,γ<sub>2</sub>,δ<sub>2</sub>,ε<sub>3</sub>-D<sub>4</sub>]-Lys (Fig. 1f), all of the 21 Lys side chain methylene proton signals are  
197 *stereo-specifically* assigned to each of the β<sub>3</sub>, γ<sub>3</sub>, δ<sub>3</sub>, and ε<sub>2</sub> <sup>1</sup>H signals, thus providing precious  
198 clues to examine the local conformations of the Lys side chains in solution.~~

### 199 **3.2 Structural information inferable from the Lys side chain chemical shifts**

200 Note that the chemical shifts in Table 1 for the 21 Lys residues in the SAIL-Lys labeled SNase  
201 variant are *not* corrected for the various isotope-induced shifts caused by the complicated isotope-  
202 labeling pattern of the SAIL-Lys structure (*see*, Fig. 1f). Based on comprehensive NMR data, we  
203 should be able to elucidate the *dual* role of the Lys side chains in terms of the conformational  
204 dynamics and functional properties of a protein in further detail, using various solution NMR

205 methods. In this section, we briefly interpret the chemical shift data to characterize the local  
 206 conformational features by the  $^1\text{H}$ ,  $^{13}\text{C}$ , and  $^{15}\text{N}$ -signals compiled in Table 1, which should be  
 207 followed by more extensive studies in the future. Although we have not yet attempted to collect  
 208 the comprehensive NOEs, such as by using a *fully* SAIL-labeled SNase variant (Kainosho et al.,  
 209 2006), it was obvious that the chemical shift data with exclusive and unambiguous assignments  
 210 for the Lys residues contain an abundance of information on the side chain conformations and  
 211 ionization states of the  $\zeta$ -amino groups. As described above, the unusual chemical shifts of the  
 212 Lys-66 side chain confirmed the deprotonated state of its  $\zeta$ -amino group. We also obtained some  
 213 interesting structural information for the other Lys residues with protonated  $\zeta$ -amino groups. For  
 214 example, the Lys-9 side chain exists in two conformational states in the crystalline state (PDB  
 215 Entry #3HZX), which only differ in the  $\chi^4$ -angle; i.e., *Form A* (*trans*,  $\sim -175^\circ$ ) and *Form B* (*gauche*<sup>+</sup>,

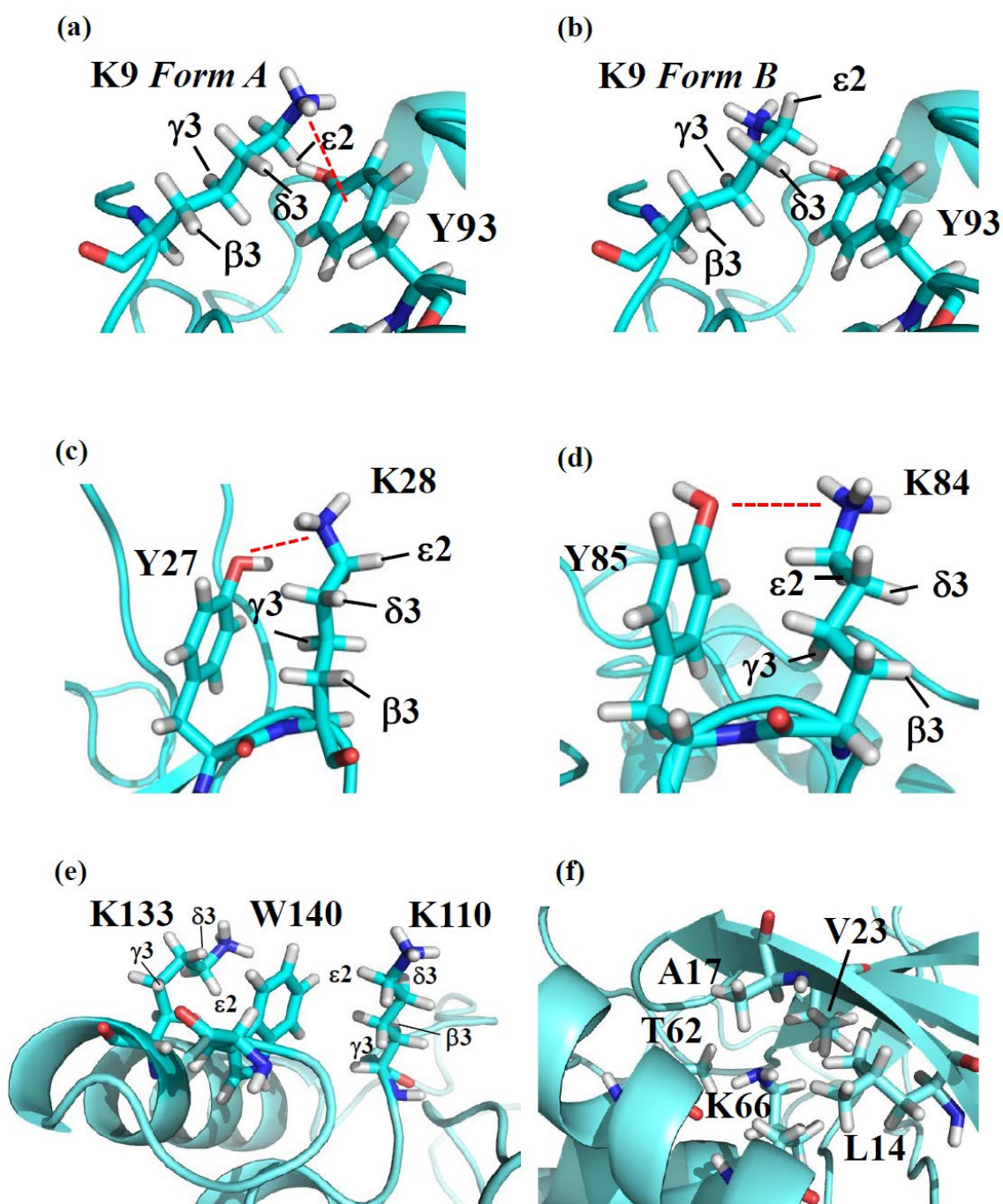
216

	$^{13}\text{C}^\alpha$	$^1\text{H}^\alpha$	$^{13}\text{C}^\beta$	$^1\text{H}^\beta$	$^{13}\text{C}^\gamma$	$^1\text{H}^\gamma$	$^{13}\text{C}^\delta$	$^1\text{H}^\delta$	$^{13}\text{C}^\epsilon$	$^1\text{H}^\epsilon$	$^{15}\text{N}^\zeta$
<b>K5</b>	56.4	4.54	32.8	1.98	24.1	1.60	29.2	1.85	41.8	3.17	n.d.
<b>K6</b>	56.0	4.54	33.3	1.97	24.5	1.63	28.4	1.86	41.8	3.17	n.d.
<b>K9</b>	55.9	5.00	34.5	1.56	25.1	1.49	28.8	1.04	40.5	1.98	30.8
<b>K16</b>	56.6	4.60	35.6	1.92	23.9	1.47	28.3	1.78	41.7	3.10	31.7
<b>K24</b>	55.8	5.61	34.3	2.10	25.2	1.54	29.5	1.77	41.5	2.98	32.0
<b>K28</b>	57.5	3.80	29.5	2.00	24.6	0.61	29.1	1.63	41.9	3.16	31.9
<b>K53</b>	59.2	3.84	31.5	1.64	24.7	1.21	28.8	1.61	41.6	2.90	31.8
<b>K63</b>	60.8	3.78	32.8	1.91	24.2	1.46	29.7	1.75	41.8	3.17	n.d.
<b>K64</b>	59.4	4.13	31.8	1.89	24.5	1.55	28.9	1.74	41.6	3.03	31.7
<b>K66</b>	59.5	4.12	32.8	1.85	25.7	1.76	34.0	1.47	43.8	2.70	20.9
<b>K70</b>	57.8	4.55	32.7	1.92	24.3	1.60	28.6	1.83	41.8	3.19	n.d.
<b>K71</b>	55.6	4.84	35.2	2.01	24.4	1.60	28.4	1.82	41.4	3.04	31.8
<b>K78</b>	57.1	4.53	33.0	2.06	24.1	1.67	28.5	1.90	42.2	3.24	31.5
<b>K84</b>	58.3	4.24	31.3	1.65	23.1	0.64	28.8	1.61	41.5	2.95	32.0
<b>K97</b>	54.2	4.81	32.9	1.89	24.6	1.62	28.7	1.79	41.8	3.19	n.d.
<b>K110</b>	54.4	5.27	35.2	2.17	25.1	1.42	29.2	1.79	41.5	2.68	31.7
<b>K116</b>	57.7	4.04	31.7	1.88	24.1	1.30	28.5	1.69	41.7	3.06	31.7
<b>K127</b>	59.3	4.31	31.9	2.12	24.9	1.77	29.1	1.83	41.7	3.12	31.4

<b>K133</b>	59.6	3.62	32.2	1.42	24.1	0.59	28.9	1.15	40.9	2.10	31.7
<b>K134</b>	59.4	4.13	32.0	2.15	24.4	1.65	29.5	1.76	41.8	3.13	31.6
<b>K136</b>	56.8	3.76	28.8	1.66	24.6	1.55	28.7	1.95	42.0	3.20	31.5
<b>Avg. <math>\delta</math> ppm</b>	-	-	<b>33.1</b>	<b>1.95</b>	<b>24.5</b>	<b>1.54</b>	<b>28.9</b>	<b>1.68</b>	<b>41.7</b>	<b>3.09</b>	<b>31.7</b>

217

218 **Table 1. The  $^1\text{H}$ ,  $^{13}\text{C}$ ,  $^{15}\text{N}$  chemical shifts for the sidechains of the 21 Lys residues in**  
 219  **$\Delta$ +PHS/V66K SNase selectively labeled with SAIL-Lys in  $\text{D}_2\text{O}$ .** The  $^1\text{H}$  and  $^{13}\text{C}$  signals were assigned  
 220 by the 3D HCCH-TOCSY experiment recorded on a Bruker 600 MHz equipment 30 °C, pH 8.0 using a 600 MHz  
 221 NMR machine. The  $^{15}\text{N}$ -signals were assigned by the HECENZ correlations and those denoted as “n.d.” were not  
 222 clearly observed. Since one of the prochiral methylene protons was stereo-specifically deuterated in the SAIL-Lys, i.e.  
 223 [ $U$ - $^{13}\text{C}$ ,  $^{15}\text{N}$ ;  $\beta_{2,\gamma_2,\delta_2,\epsilon_3}$ - $\text{D}_4$ ]-Lys, thus the observed  $^1\text{H}$ -signals were unambiguously assigned. The chemical shifts for  
 224 the engineered Lys-66, which has a deprotonated  $\zeta$ -amino group, are shown italic. The averaged chemical shifts are  
 225 obtained by excluding some of the **outlying** shifts, and the measurement errors were estimated as less than 0.2 and  
 226 0.02 ppm, for  $^{13}\text{C}/^{15}\text{N}$ - and  $^1\text{H}$ -chemical shifts, respectively. All chemical shifts are not corrected for the isotope shifts.



227  
 228 **Figure 2: The local structures around the Lys residues, which exhibit unusual side chain**  
 229 **chemical shifts, in the crystal structure of the SNase variant (PDB: 3HZX).** The crystal structure  
 230 of the SNase variant was solved as a complex with calcium ions and thymidine 3',5'-diphosphate. Therefore,

231 it may be slightly different from that in the free state. The figures were created with the PyMOL 2.4 software  
232 in order to highlight the relative orientations between the Lys side chains and nearby aromatic rings (a)-(e),  
233 and Lys-66 and the surrounding hydrophobic amino acids (f). The nomenclatures of the prochiral hydrogen  
234 atoms, shown as the suffixes in the figures, are according to the recommended atom identifiers (Markley et  
235 al., 1998).

236 ~~methods. In this section, we briefly interpret the chemical shift data to characterize the local~~  
237 ~~conformational features by the  $^1\text{H}$ ,  $^{13}\text{C}$ , and  $^{15}\text{N}$  signals compiled in Table 1, which should be~~  
238 ~~followed by more extensive studies in the future. Although we have not yet attempted to collect~~  
239 ~~the comprehensive NOEs, such as by using a fully SAHL labeled SNase variant (Kainosho et al.,~~  
240 ~~2006), it was obvious that the chemical shift data with exclusive and unambiguous assignments~~  
241 ~~for the Lys residues contain an abundance of information on the side chain conformations and~~  
242 ~~ionization states of the  $\zeta$  amino groups. As described above, the unusual chemical shifts of the~~  
243 ~~Lys-66 side chain confirmed the deprotonated state of its  $\zeta$  amino group. We also obtained some~~  
244 ~~interesting structural information for the other Lys residues with protonated  $\zeta$  amino groups. For~~  
245 ~~example, the Lys-9 side chain exists in two conformational states in the crystalline state (PDB~~  
246 ~~Entry #3HZX), which only differ in the  $\chi^4$  angle; i.e., *Form A* (*trans*,  $\sim 175^\circ$ ) and *Form B* (*gauche*<sup>+</sup>,~~  
247  $\sim +44^\circ$ ), as shown in Fig. 2a and b, respectively (*see also*, Table A1). The significantly up-field  
248 shifted signals observed for Lys-9 relative to the averaged chemical shifts ( $\Delta\delta$ , ppm) are obviously  
249 due to the aromatic ring current of Tyr-93; i.e.,  $^{15}\text{N}^\zeta$  (30.8 ppm,  $\Delta\delta = -0.9$  ppm),  $^{13}\text{C}^\epsilon/{}^1\text{H}^\epsilon$  (40.5/1.98  
250 ppm,  $\Delta\delta = -1.2/-1.11$  ppm) and  ${}^1\text{H}^{\delta^3}$  (1.04 ppm,  $\Delta\delta = -0.64$  ppm). These chemical shifts suggest the  
251  $\zeta\text{-NH}^{3+}$ - $\pi$  interaction, as shown by the dashed red line (Fig. 2a). Therefore, the chemical shifts for  
252 Lys-9 strongly imply that the van der Waals interactions between the aliphatic side chain, as well  
253 as the *electrostatic interaction* between the positively charged  $\zeta\text{-HN}^{3+}$  and the nearby aromatic  
254 ring of Tyr-93, simultaneously contribute to preferentially stabilize the *Form A* conformation in  
255 solution (Fig. 2a).

256 The high-field shifts of the side chain methylenes, induced by the neighboring aromatic rings,  
257 were also detected for Lys-28, Lys-84 and Lys-133. Considering the local structures of Lys-28 and  
258 Lys-84 in the crystal (Fig. 2c, d), the relative orientations between Lys-28 and Tyr-27, and Lys-84  
259 and Tyr-85 seem to be similar to those in the crystal, and are responsible for the large high-field  
260 shifts for only their  ${}^1\text{H}^{\gamma^3}$  signals; i.e., Lys-28: 0.61 ppm,  $\Delta\delta = -0.93$  ppm; Lys-84: 0.64 ppm,  $\Delta\delta = -$

261 0.90 ppm, while the other  $^{13}\text{C}/^1\text{H}$  shifts remain within the average ranges (Table 1). The small but  
262 obvious low-field shifts for the  $^{15}\text{N}^\zeta$  (Lys-28, Lys-84: 32.0 ppm,  $\Delta\delta = +0.3$  ppm) might be caused  
263 by the electrostatic interactions between the  $\text{O}^\eta$  of Tyr-27/Tyr-85 and the  $\text{N}^\zeta$  of Lys-28/Lys-84,  
264 respectively, as shown by the dashed red lines (Fig. 2 c, d). The bulky indole ring of Trp-140 seems  
265 to simultaneously stabilize the aliphatic chains of both Lys-133 and Lys-110, inducing the high-  
266 field shifts for some of the side chain signals; i.e., Lys-133  $^{13}\text{C}^\varepsilon/^1\text{H}^{\varepsilon 2}$  (40.9/2.10 ppm,  $\Delta\delta = -0.8/-$   
267 0.99 ppm),  $^1\text{H}^{\delta 3}$  (1.15 ppm,  $\Delta\delta = -0.53$  ppm),  $^1\text{H}^{\gamma 3}$  (0.59 ppm,  $\Delta\delta = -0.95$  ppm) and  $^1\text{H}^{\beta 3}$  (1.42 ppm,  
268  $\Delta\delta = -0.53$  ppm); Lys-110  $^1\text{H}^{\varepsilon 2}$  (2.68 ppm,  $\Delta\delta = -0.41$  ppm). These up-field shifted signals indicate  
269 that **the van der Waals interactions** between the methylene moieties of Lys-133 and Lys-110, with  
270 the hydrophobic indole ring of Trp-140 sandwiched in the middle, are also preserved in solution  
271 (Fig. 2e). Interestingly, the chemical shift differences between the two prochiral methylene protons  
272 attached to the  $\varepsilon$ -carbons of the Lys residues, observed for the SNase variant residue-selectively  
273 labeled with  $[\text{U}-^{13}\text{C}, ^{15}\text{N}]$ -Lys, are only considerably large for the Lys-110 and -133 residues, while  
274 those for the other 19 Lys residues were much smaller than  $\sim 0.05$  ppm, if present (Fig. A3). Since  
275 the  $^1\text{H}^{\varepsilon 2}$  chemical shifts were observed at 0.15 and 0.17 ppm higher field than the  $^1\text{H}^{\varepsilon 3}$  chemical  
276 shifts for Lys-110 and -133, respectively, the conformations of these two Lys residues are likely to  
277 be similar to those in the crystal (Fig. 2e).

278 On the other hand, the striking chemical shifts observed for the Lys-66 residue, which is  
279 deliberately trapped within the hydrophobic environment engineered in the SNase variant (Fig. 2f),  
280 clearly reveal the strong influence of the ionization state of the  $\zeta$ -amino group on the Lys side  
281 chain chemical shifts. As shown in Table 1, the  $^{15}\text{N}^\zeta$  chemical shift of the  $\zeta$ - $\text{ND}_2$  of Lys-66 in the  
282 SNase variant appears at an unusually high-field position, as compared to the averaged chemical  
283 shift range for the  $\zeta$ - $\text{ND}^{3+}$  in the other Lys residues; i.e.,  $^{15}\text{N}^\zeta$  (Lys-66: 20.9 ppm,  $\Delta\delta = -10.8$  ppm),  
284 which is close to the value of the  $\zeta$ - $\text{NH}_2$  chemical shift, 23.3 ppm, previously reported for Lys-66  
285 in the  $[\text{U}-^{13}\text{C}, ^{15}\text{N}]$ -SNase variant (André et al., 2007; Takayama et al., 2008). Apparently, the  $^{15}\text{N}^\zeta$   
286 chemical shifts provide a quite useful clue to distinguish between the deprotonated and protonated  
287  $\zeta$ -amino groups of Lys **residues. However, the** complete side chain assignment including the  
288 terminal  $\zeta$ - $^{15}\text{N}$  signals by conventional methods using a  $[\text{U}-^{13}\text{C}, ^{15}\text{N}]$ -protein is usually laborious,  
289 and occasionally impossible.

290 The deprotonation of the  $\zeta$ -amino group caused sizable  $^1\text{H}$  and  $^{13}\text{C}$  chemical shift changes  
291 down to the  $\gamma$ -position in the side chain, as observed for Lys-66; i.e.,  $^{13}\text{C}^\epsilon/{}^1\text{H}^\epsilon$  (43.8/2.70 ppm,  
292  $\Delta\delta = +2.1/-0.39$  ppm),  $^{13}\text{C}^\delta/{}^1\text{H}^\delta$  (34.0/1.47 ppm,  $\Delta\delta = +5.1/-0.21$  ppm), and  $^{13}\text{C}^\gamma/{}^1\text{H}^\gamma$  (25.7/1.76  
293 ppm,  $\Delta\delta = +1.2/+0.22$  ppm). These *deprotonation* shifts, especially on the  $^{13}\text{C}^\epsilon$  and/or  $^{13}\text{C}^\delta$  chemical  
294 shifts, could therefore be used as a useful alternative index to characterize the ionization states of  
295 the  $\zeta$ -amino groups of Lys residues in a protein, since they can be accurately and readily observed  
296 and assigned by using a protein selectively labeled with SAIL-Lys. It should be noted, however,  
297 that the side chain chemical shifts in general might significantly vary according to the local  
298 environments, such as the relative position to aromatic rings, and thus the results obtained  
299 exclusively from the side chain chemical shifts might not be absolutely reliable. To avoid any  
300 possible uncertainties in characterizing the ionization states of  $\zeta$ -amino groups, an alternative  
301 approach using the deuterium-induced isotope shifts of the SAIL-Lys side chain  $^{13}\text{C}$  signals must  
302 be developed.

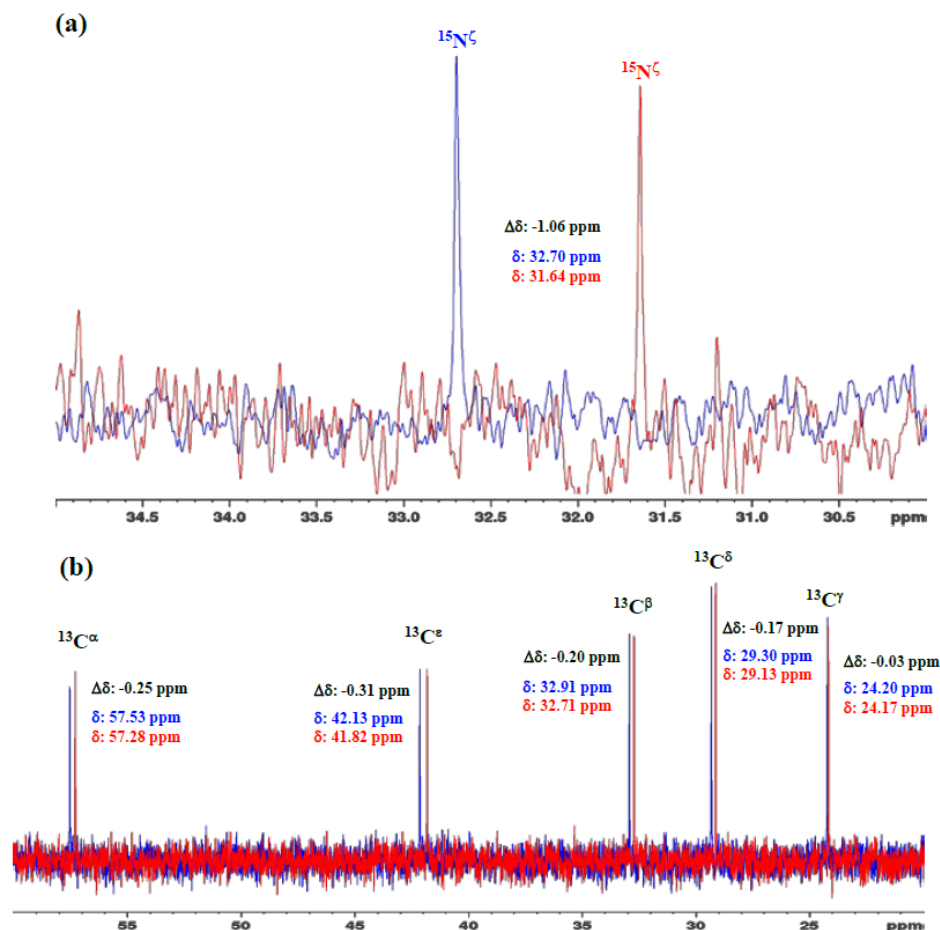
### 303 **3.3 Characterization of the ionization state of the $\zeta$ -amino group of Lys residues using the** 304 **effects of deuterium-induced isotope shifts on the side chain $^{13}\text{C}$ and $^{15}\text{N}$ signals**

305 In our previous studies investigating the effects of the deuterium-induced isotope shifts on  
306 the  $^{13}\text{C}$  signals adjacent to polar functional groups with an exchangeable hydrogen, such as  
307 hydroxyl (OH) or sulfhydryl (SH) groups, we demonstrated that those isotope shifts are versatile  
308 indices for identifying residues, such as Tyr, Thr, Ser or Cys, with *exceptionally* slow hydrogen  
309 exchange rates (Takeda et al., 2014). For example, in a protein selectively labeled with [ $\zeta$ - $^{13}\text{C}$ ]-  
310 Tyr, the Tyr residues have much slower hydrogen exchange rates for the  $\eta$ -hydroxyl groups than  
311 the isotope shift differences in the  $^{13}\text{C}^\zeta$  signals, and exhibit well-resolved pairwise signals with  
312 nearly equal intensities in the 1D  $^{13}\text{C}$ -NMR spectrum in  $\text{H}_2\text{O}$ - $\text{D}_2\text{O}$  (1:1) (Takeda et al., 2009). The  
313 up- and downfield counterparts of the pairwise  $^{13}\text{C}^\zeta$  signals correspond to those in  $\text{D}_2\text{O}$  and  $\text{H}_2\text{O}$ ,  
314 respectively, and their relative intensities reflect the fractionation factors; i.e.,  $[\text{OD}]/[\text{OH}]$ . Similar  
315 approaches have been developed for Ser, Thr and Cys residues, using the  $^{13}\text{C}^\beta$  signals observed for  
316 proteins selectively labeled with [ $\beta$ - $^{13}\text{C}$ ;  $\beta$ ,  $\beta$ - $\text{D}_2$ ]-Ser, [ $\beta$ - $^{13}\text{C}$ ;  $\beta$ -D]-Thr, and [ $\beta$ - $^{13}\text{C}$ ;  $\beta$ ,  $\beta$ - $\text{D}_2$ ]-Cys,  
317 respectively (Takeda et al., 2010, 2011). Since the isolated  $^{13}\text{C}^\beta(\text{D}_2)$  or  $^{13}\text{C}^\beta(\text{D})$  moieties in the

318 labeled amino acids give extremely narrow signals under the deuterium decoupling, the  $^{13}\text{C}$ -NMR  
319 signals can be obtained with remarkably high sensitivities, especially with a  $^{13}\text{C}$ -direct observing  
320 cryogenic probe. Interestingly, while the fractionation factors for the Ser and Thr hydroxyl groups;  
321 i.e.,  $[\text{OD}]/[\text{OH}]$ , are usually close to unity, as also for the Tyr residues, those for the Cys sulfhydryl  
322 groups; i.e.,  $[\text{SD}]/[\text{SH}]$ , are around 0.4-0.5 (Takeda et al., 2010, 2011). The methods are especially  
323 important, since the functional groups of the residues readily identified as having exceptionally  
324 slow hydrogen exchange rates are most likely to be involved in hydrogen bonding networks and/or  
325 located in distinctive local environments.

326 Although the idea of estimating the hydrogen exchange rates by the deuterium-induced  
327 isotope shifts on the  $^{13}\text{C}$  nuclei adjacent to functional groups with exchangeable hydrogens was  
328 originally exploited years ago, for the backbone amide groups in the residue-selectively labeled  
329 proteins with  $[\text{C}'\text{-}^{13}\text{C}]$ -amino acid(s) (Kainosho and Tsuji 1982; Markley and Kainosho, 1993), it  
330 has not yet been applied for the Lys  $\zeta$ -amino groups. Having established the complete assignment  
331 for the 21 Lys residues in the SNase variant selectively labeled with SAIL-Lys (Table 1), we next  
332 examined the deuterium-induced chemical shifts in detail for the Lys side chain signals. In the case  
333 of Lys residues, the NMR signals of the  $\zeta$ -amino  $^{15}\text{N}$  and  $\epsilon$ - or  $\delta$ -carbon  $^{13}\text{C}$  signals would be  
334 plausible candidates for probing the deuterium substitution effects. There have only been a few  
335 reports on the isotope shifts of the  $\delta$ - and  $\epsilon$ - $^{13}\text{C}$  for the Lys-residues induced by the deuteration of  
336  $\zeta$ -amino groups (Hansen, 1983; Dziembowska et al., 2004). However, apparently no  
337 comprehensive studies have applied the deuterium-induced isotope shifts to characterize the  
338 ionization states of Lys residues.

339 We first examined the 1D  $^{13}\text{C}$ - and  $^{15}\text{N}$ -NMR spectra of  $[\text{}^{15}\text{N}_2]$ -Lys in  $\text{D}_2\text{O}$  and  $\text{H}_2\text{O}$ , at pH 8 and  
340 30 °C, to choose the suitable NMR probes to distinguish between the deprotonated and  
341 protonated  $\zeta$ -amino groups (Fig. 3). The  $\zeta$ - $^{15}\text{N}$  signal appears at  $\sim 1$  ppm up-field in  $\text{D}_2\text{O}$  relative  
342 to that in  $\text{H}_2\text{O}$  (Fig. 3a), and the aliphatic  $^{13}\text{C}$  signals of  $[\text{}^{15}\text{N}_2]$ -Lys at the natural abundance also  
343 showed isotope shifts,  $\Delta\delta[^{13}\text{C}^i \text{ (in } \text{D}_2\text{O}) - \delta^{13}\text{C}^i \text{ (in } \text{H}_2\text{O})]$ ; i.e.,  $^{13}\text{C}^\alpha$ , -0.25 ppm;  $^{13}\text{C}^\beta$ , -0.20 ppm;  
344  $^{13}\text{C}^\gamma$ , -0.03 ppm;  $^{13}\text{C}^\delta$ , -0.17 ppm; and  $^{13}\text{C}^\epsilon$ , -0.31 ppm (Fig. 3b). Although the isotope shifts for

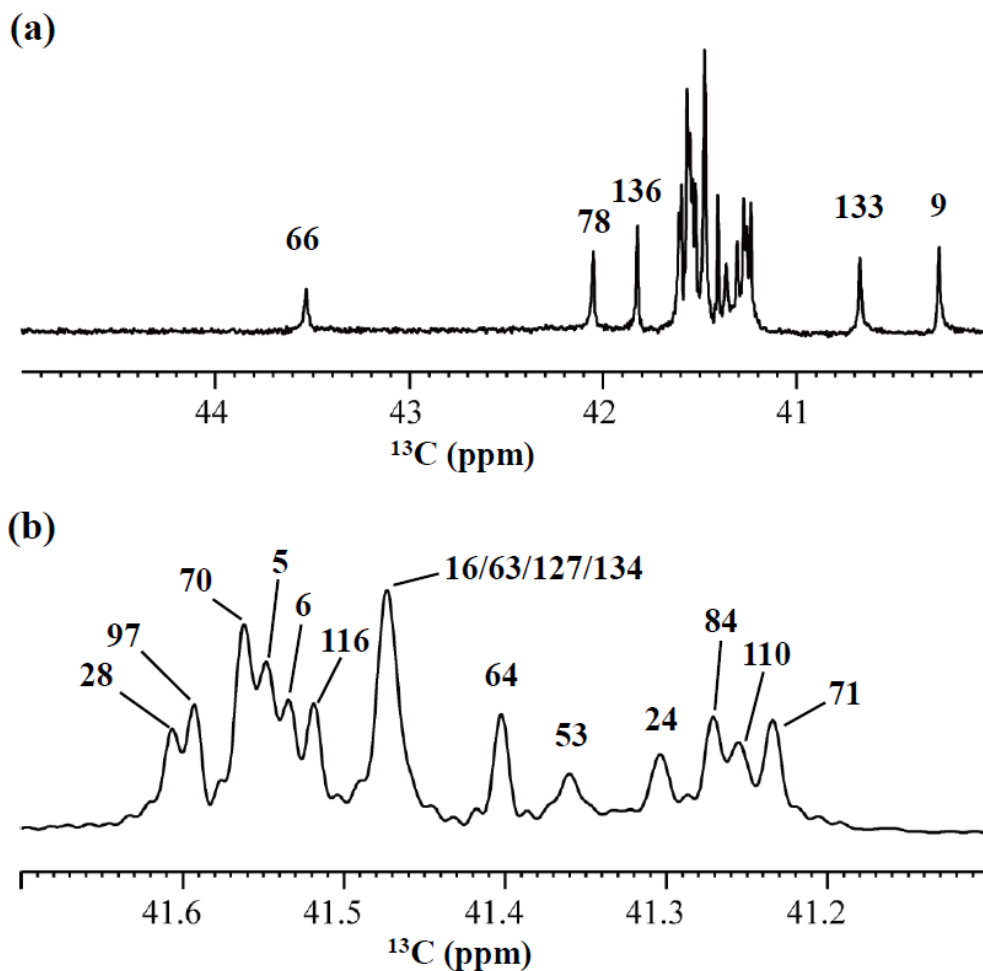


345  
 346 **Figure 3: 1D  $^{15}\text{N}$ - and  $^{13}\text{C}$ -NMR spectra of  $[\text{}^{15}\text{N}_2]$ -lysine free in  $\text{H}_2\text{O}$  and  $\text{D}_2\text{O}$ .** The 96.3 MHz  
 347 1D  $^{15}\text{N}$ -NMR spectra (Figure 3a) and 239.0 MHz 1D  $^{13}\text{C}$ -NMR spectra (Figure 3b) of  $[\text{}^{15}\text{N}_2]$ -lysine were  
 348 measured at 30 °C on a Bruker Avance III 950 spectrometer with a TCI cryogenic probe, using ~70 mM  
 349 solutions of either 20 mM Tris buffer prepared with  $\text{H}_2\text{O}$  (or  $\text{D}_2\text{O}$ ) at pH (or pD) 8.0. The NMR spectra and  
 350 the chemical shifts,  $\delta$  ppm, shown in blue and red, are those for the  $\text{H}_2\text{O}$  and  $\text{D}_2\text{O}$  buffer solutions,  
 351 respectively. The deuterium-induced shifts,  $\Delta\delta$  ppm :  $\delta$  (in  $\text{D}_2\text{O}$ ) -  $\delta$  (in  $\text{H}_2\text{O}$ ) for the  $^{15}\text{N}_\zeta$  and side chain  $^{13}\text{C}$   
 352 signals are shown in black.

353  $^{13}\text{C}_\alpha$  and  $^{13}\text{C}_\beta$  are due to the deuteration of the  $\alpha$ -amino group, those for  $^{13}\text{C}_\delta$  and  $^{13}\text{C}_\epsilon$  are obviously  
 354 due to the deuteration of the  $\zeta$ -amino group. Considering the finding that the  $^{13}\text{C}_\epsilon$  of Lys gives an  
 355 isolated signal far from the others and exhibits a ~1.8-fold larger isotope shift as compared to  $^{13}\text{C}_\delta$ ,

356 the  $^{13}\text{C}^\epsilon$  and  $^{15}\text{N}^\zeta$  signals seem to be good candidates for probing the ionization states of Lys  
357 residues in the SNase variant.

358 Although the  $^{15}\text{N}^\zeta$  and  $^{13}\text{C}^\epsilon$  chemical shifts for the Lys residues can be measured by the HECENZ  
359 and  $^1\text{H}$ - $^{13}\text{C}$  ct-HSQC experiments, respectively, using the SNase variant selectively



360  
361 **Figure 4: 125.7 MHz  $\{^1\text{H}, ^2\text{D}\}$ -decoupled 1D- $^{13}\text{C}$ -NMR spectrum for the SNase variant**  
362 **selectively labeled with  $[\epsilon\text{-}^{13}\text{C}; \epsilon, \epsilon\text{-D}_2]\text{-Lys}$ .** The spectra were measured at 25 °C, pH 8.0, in  $\text{D}_2\text{O}$   
363 solution on an Avance 500 spectrometer equipped with a DCH cryogenic probe. Although only a  
364 few discrete  $^{13}\text{C}^\epsilon$  signals are apparent in Figure 4a, the congested spectral region around 41-42 ppm  
365 shows well-separated signals due to their narrow line-widths of 1-2 Hz (Figure 4b). **All of the 1D**  
366 **NMR signals for  $^{13}\text{C}^\epsilon$  were readily assigned by using the chemical shift data obtained from the 3D**  
367 **HCCH TOCSY experiment for the SNase variant selectively labeled with SAIL-Lys (see Sect. 3.1).**

368 labeled with [U-<sup>13</sup>C, <sup>15</sup>N]-Lys or SAIL-Lys, it was rather difficult to determine the accurate isotope  
 369 shifts of the <sup>15</sup>N $\zeta$  and <sup>13</sup>C $\epsilon$  signals for all 21 Lys residues by these methods. Especially, the accurate  
 370 chemical shift measurement for an individual <sup>13</sup>C $\epsilon$  signal was hampered by the insufficient quality

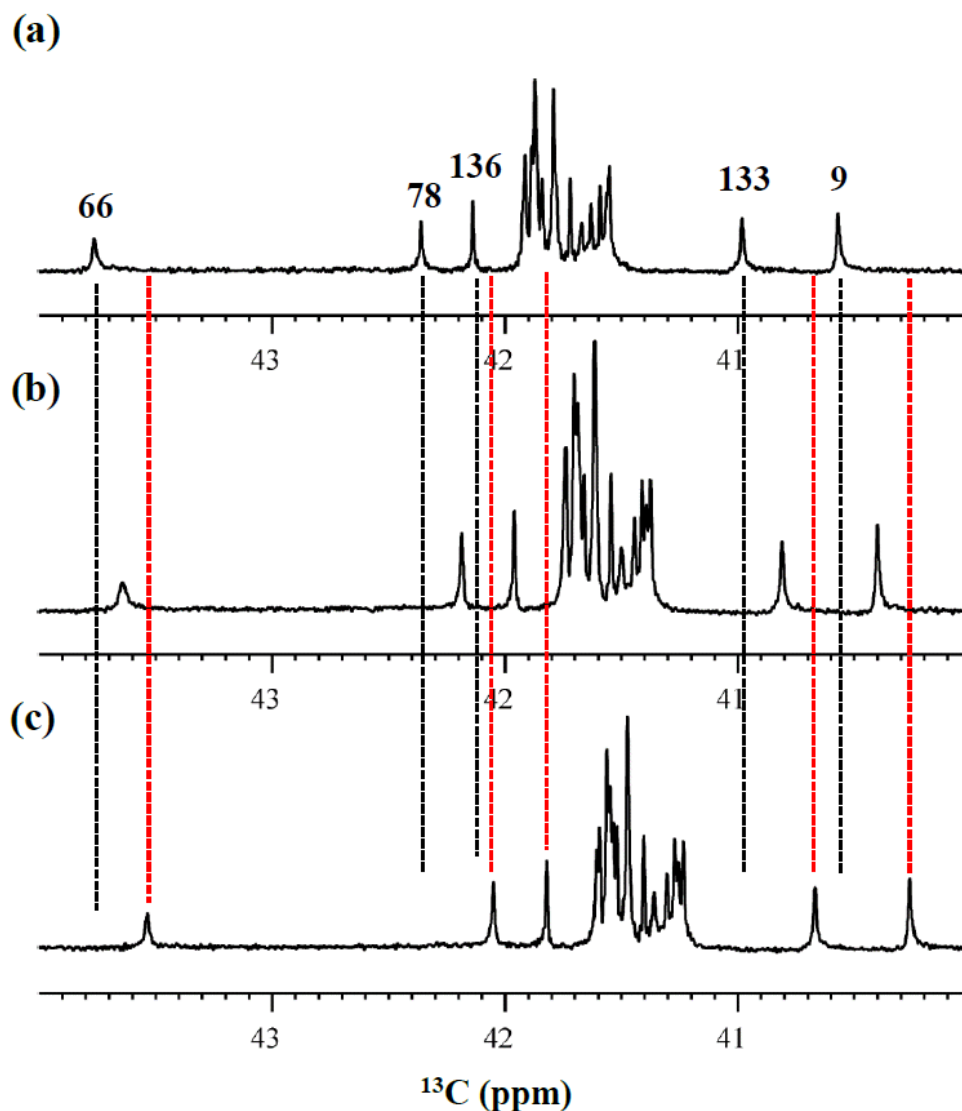
	$\delta^{15}\text{N}\zeta$ in H <sub>2</sub> O	$\delta^{15}\text{N}\zeta$ in D <sub>2</sub> O	$\Delta\delta^{15}\text{N}\zeta$ ppm	$\delta^{13}\text{C}\epsilon$ in H <sub>2</sub> O	$\delta^{13}\text{C}\epsilon$ in D <sub>2</sub> O	$\Delta\delta^{13}\text{C}\epsilon$ ppm
<b>K5</b>	n.d.	n.d.	n.d.	41.89	41.54	-0.35
<b>K6</b>	n.d.	n.d.	n.d.	41.87	41.53	-0.34
<b>K9</b>	31.9	30.8	-1.1	40.55	40.26	-0.29
<b>K16</b>	32.9	31.8	-1.1	41.80	41.47	-0.33
<b>K24</b>	33.1	31.8	-1.3	41.66	41.31	-0.35
<b>K28</b>	33.0	32.0	-1.0	41.92	41.62	-0.30
<b>K53</b>	32.9	31.8	-1.1	n.d.	41.36	n.d.
<b>K63</b>	n.d.	n.d.	n.d.	41.80	41.47	-0.33
<b>K64</b>	32.7	31.7	-1.0	41.72	41.41	-0.31
<b>K66</b>	22.7	20.9	-1.8	43.75	43.54	-0.21
<b>K70</b>	n.d.	n.d.	n.d.	41.89	41.55	-0.34
<b>K71</b>	32.8	31.8	-1.0	41.55	41.24	-0.31
<b>K78</b>	32.7	31.5	-1.2	42.37	42.09	-0.28
<b>K84</b>	33.1	32.0	-1.1	41.64	41.36	-0.28
<b>K97</b>	n.d.	n.d.	n.d.	41.91	41.59	-0.32
<b>K110</b>	32.8	31.6	-1.2	41.65	41.26	-0.39
<b>K116</b>	32.8	31.7	-1.1	41.86	41.52	-0.34
<b>K127</b>	32.6	31.4	-1.2	41.80	41.50	-0.30
<b>K133</b>	32.8	31.7	-1.1	40.96	40.67	-0.29
<b>K134</b>	32.6	31.6	-1.0	41.80	41.50	-0.30
<b>K136</b>	32.5	31.5	-1.0	42.12	41.82	-0.30
Avg. $\delta$ , $\Delta\delta$ ppm	32.7	31.6	-1.1 +/- 0.1	41.72	41.40	-0.32 +/- 0.02

371 **Table 2. Deuterium-induced isotope shifts for the sidechain <sup>15</sup>N $\zeta$  and <sup>13</sup>C $\epsilon$  signals of the 21**  
 372 **Lys residues in  $\Delta$ +PHS/V66K SNase.** The <sup>15</sup>N $\zeta$  and <sup>13</sup>C $\epsilon$  chemical shift data in H<sub>2</sub>O and D<sub>2</sub>O were obtained  
 373 for the SNase labeled either with SAIL-Lys or [ $\epsilon$ -<sup>13</sup>C;  $\epsilon$ , $\epsilon$ -D<sub>2</sub>]-Lys, respectively. Note that the 1D <sup>13</sup>C $\epsilon$  data measured  
 374 at 125.7 MHz the 1D <sup>13</sup>C-spectra are much higher precision as compared to those by the 2D HSQC using the SNase  
 375 labeled with SAIL-Lys. **The averaged chemical shifts in the last row are obtained for the Lys residues with protonated**

376  $\zeta$ -amino groups, except for Lys-66 (italic) which has a deprotonated  $\zeta$ -amino group. The averaged  $\Delta\delta$  values show the  
377 difference between the averaged  $^{15}\text{N}^\zeta$  and  $^{13}\text{C}^\epsilon$ , except for Lys-66 which are the difference between its  $^{15}\text{N}^\zeta$  and  $^{13}\text{C}^\epsilon$   
378 shifts in  $\text{H}_2\text{O}$  and  $\text{D}_2\text{O}$ . Negative  $\Delta\delta$  values indicate the chemical shifts in  $\text{D}_2\text{O}$  are up-field shifted due to deuteration  
379 of the  $\zeta$ -amino groups.

380 of the ct-HSQC spectrum, even for the protein labeled with SAIL-Lys (Fig. A3). Therefore, we  
381 used  $[\epsilon\text{-}^{13}\text{C}; \epsilon, \epsilon\text{-D}_2]$ -Lys to reduce the line-widths of the  $^{13}\text{C}^\epsilon$  signals for the Lys-residues in the  
382 SNase variant. As expected, the 1D  $^{13}\text{C}$ -NMR spectra of the SNase variant selectively labeled with  
383  $[\epsilon\text{-}^{13}\text{C}; \epsilon, \epsilon\text{-D}_2]$ -Lys showed remarkably well-resolved signals with line-widths less than 2 Hz,  
384 under the  $^1\text{H}/^2\text{D}$  double decoupling conditions (Fig. 4). Note that the weak background signals due  
385 to the naturally abundant  $^{13}\text{C}$  nuclei were filtered out in this spectrum (Fig. A2). By referring to  
386 the chemical shifts in Table 1, which were determined by the 3D HCCH TOCSY experiment for  
387 the SNase labeled with SAIL-Lys, all of the 1-D  $^{13}\text{C}^\epsilon$  signals were unambiguously assigned (Fig.  
388 4 a, b). The chemical shifts of  $^{13}\text{C}^\epsilon$  are slightly different among the data sets, because the isotope  
389 shifts induced by the nearby isotopes on the  $^{13}\text{C}^\epsilon$  signals are different for SAIL-Lys and  $[\epsilon\text{-}^{13}\text{C}; \epsilon,$   
390  $\epsilon\text{-D}_2]$ -Lys (Tables 1, 2). The  $^{13}\text{C}^\epsilon$  chemical shifts in  $\text{H}_2\text{O}$  and  $\text{D}_2\text{O}$ , which were accurately  
391 determined by the 1D  $^{13}\text{C}$ -NMR spectra, are presented in Fig. 5. At a glance, the  $^{13}\text{C}^\epsilon$  spectra in  
392 Fig. 5a and 5c look almost the same, since the signals moved up-field with a constant increment  
393 of  $-0.32 \pm 0.02$  ppm, except for the  $^{13}\text{C}^\epsilon$  signal of Lys-66 (Table 2). Since the  $\delta^{13}\text{C}^\epsilon$  values in  $\text{H}_2\text{O}$   
394 and  $\text{D}_2\text{O}$  are very close to those for the *free*  $^{15}\text{N}_2$ -Lys (Fig. 3b), the  $\zeta$ -amino groups are protonated  
395 in  $\text{H}_2\text{O}$  and deuterated in  $\text{D}_2\text{O}$ , and thus the averaged deuterium-induced isotope shift was  
396 designated as  $\Delta\delta^{13}\text{C}^\epsilon$  [ $\text{N}^\zeta\text{D}_3^+ - \text{N}^\zeta\text{H}_3^+$ ]. Similarly, the averaged  $\Delta\delta^{15}\text{N}^\zeta$  [ $\text{N}^\zeta\text{D}_3^+ - \text{N}^\zeta\text{H}_3^+$ ], excluding the  
397 value for Lys-66, was determined to be  $-1.1 \pm 0.1$  ppm, which was also close to the *free*  $^{15}\text{N}_2$ -  
398 Lys (Fig. 3a). The  $\Delta\delta^{13}\text{C}^\epsilon$  and  $\Delta\delta^{15}\text{N}^\zeta$  for Lys-66, which are  $-0.21$  and  $-1.8$  ppm (Table 2),  
399 respectively, confirmed that the  $\zeta$ -amino group of this residue is deprotonated at pH 8, and should  
400 be designated as  $\Delta\delta^{13}\text{C}^\epsilon$  [ $\text{N}^\zeta\text{D}_2 - \text{N}^\zeta\text{H}_2$ ] and  $\Delta\delta^{15}\text{N}^\zeta$  [ $\text{N}^\zeta\text{D}_2 - \text{N}^\zeta\text{H}_2$ ]. Interestingly, the fact that the  
401 averaged  $\Delta\delta^{13}\text{C}^\epsilon$  [ $\text{N}^\zeta\text{D}_3^+ - \text{N}^\zeta\text{H}_3^+$ ],  $-0.32$  ppm, was  $\sim 1.5$  times larger than the  $\Delta\delta^{13}\text{C}^\epsilon$  [ $\text{N}^\zeta\text{D}_2 - \text{N}^\zeta\text{H}_2$ ]  
402 for Lys-66,  $-0.21$  ppm, might suggest that the deuterium-induced isotope shift on  $^{13}\text{C}^\epsilon$  is  
403 proportional to the number of hydrogen atoms on the  $\zeta$ -amino groups. In contrast, the averaged  
404  $\Delta\delta^{15}\text{N}^\zeta$  [ $\text{N}^\zeta\text{D}_3^+ - \text{N}^\zeta\text{H}_3^+$ ],  $-1.1$  ppm, was much smaller than that of the  $\Delta\delta^{15}\text{N}^\zeta$  [ $\text{N}^\zeta\text{D}_2 - \text{N}^\zeta\text{H}_2$ ] for Lys-66,  $-$   
405  $1.8$  ppm.

406 We also measured the 1D  $^{13}\text{C}$ -NMR spectrum of the SNase variant selectively labeled with  $[\epsilon\text{-}^{13}\text{C};$   
407  $\epsilon, \epsilon\text{-D}_2]$ -Lys in  $\text{H}_2\text{O}\text{-D}_2\text{O}$  (1:1), to search for the Lys residues with slowly exchanging  $\zeta$ -amino  
408 groups. Obviously, there are no such residues in the SNase variant at pH 8 and 30  $^\circ\text{C}$ , as



409  
410 **Figure 5: Isotope shifts on the  $^{13}\text{C}^\epsilon$  signals of the Lys residues in the SNase variant selectively**  
411 **labeled with  $[\epsilon\text{-}^{13}\text{C};\epsilon,\epsilon\text{-D}_2]$ -Lys, caused by the deuterium substitutions for the  $\zeta$ -amino**  
412 **groups.** The 125.7 MHz  $\{^1\text{H}, ^2\text{D}\}$ -decoupled 1D  $^{13}\text{C}$  NMR spectra were measured at 25  $^\circ\text{C}$ , pH  
413 8.0, in either  $\text{H}_2\text{O}$  (Figure 5a),  $\text{H}_2\text{O}:\text{D}_2\text{O}$  (1:1) (Figure 5b), or  $\text{D}_2\text{O}$  (Figure 5c) solutions on an  
414 Avance 500 spectrometer equipped with a DCH cryogenic probe in  $\text{H}_2\text{O}$  (a),  $\text{H}_2\text{O}:\text{D}_2\text{O}$  (1:1) (b),

415 and D<sub>2</sub>O (c) solutions. The vertical black and red dotted lines show the chemical shifts observed  
416 in 100% H<sub>2</sub>O and D<sub>2</sub>O, respectively. The complete data for the deuterium-induced isotope shifts  
417 for the sidechain <sup>15</sup>N<sup>ζ</sup> and <sup>13</sup>C<sup>ε</sup> signals are summarized in Table 2.

418 shown in Fig. 5b. Due to the rapid hydrogen exchange rates for all 21 Lys residues in this  
419 protein, the observed isotope shifts on <sup>13</sup>C<sup>ε</sup> were exactly half of the  $\Delta\delta^{13}\text{C}^\epsilon$  [ $\text{N}^\zeta\text{D}_2\text{-N}^\zeta\text{H}_2$ ] for Lys-  
420 66 or  $\Delta\delta^{13}\text{C}^\epsilon$  [ $\text{N}^\zeta\text{D}_3^+\text{-N}^\zeta\text{H}_3^+$ ] for the rest of the Lys residues. The hydrogen exchange rate constant  
421 ( $k_{ex}$ ) for the ζ-amino group of Lys-66 in the SNase variant, which is deeply embedded in the  
422 hydrophobic cavity originally occupied by Val-66 in the wild-type SNase, was 93±5 s<sup>-1</sup> at pH 8  
423 and -1 °C (Takayama et al., 2008). Therefore, the hydrogens on the ζ-amino groups in all 21 Lys  
424 residues in the SNase variant are rapidly exchanging, and thus the observed chemical shifts for the  
425 <sup>13</sup>C<sup>ε</sup> of Lys-66 and the rest of the Lys residues in H<sub>2</sub>O-D<sub>2</sub>O (1:1) are the time-averages for three  
426 isotopomers, NH<sub>2</sub>, NHD, and ND<sub>2</sub>, with nearly a 1:2:1 ratio for Lys-66, and for four isotopomers,  
427 NH<sub>3</sub><sup>+</sup>, NH<sub>2</sub>D<sup>+</sup>, NHD<sub>2</sub><sup>+</sup>, and ND<sub>3</sub><sup>+</sup>, with a ratio of 1:3:3:1. Since the time-averaged signals for Lys-  
428 66 and other Lys residues in H<sub>2</sub>O-D<sub>2</sub>O (1:1) appeared exactly in the middle of the spectra observed  
429 in H<sub>2</sub>O and D<sub>2</sub>O (Fig. 5a, c), the fractional factors for the isotopomers are nearly identical, as  
430 statistically random distributions.

#### 431 **4 Conclusions**

432 In this article, we have shown that comprehensive NMR information can be obtained by the  
433 cutting-edge isotope-aided NMR technologies for the Lys side chain moieties, comprising a long  
434 *hydrophobic* methylene chain and a *hydrophilic* ζ-amino group, to facilitate hitherto unexplored  
435 investigations toward elucidating the *dual* nature of the Lys residues in a protein. The  
436 unambiguously assigned <sup>13</sup>C signals, together with the stereo-specifically assigned prochiral  
437 protons for each of the long consecutive methylene chains, which first became available by the  
438 stereo-array isotope labeling (SAIL) method, provide unprecedented opportunities to examine the  
439 conformational features around the Lys residues in detail. The ionization states of the ζ-amino  
440 groups of Lys residues, which play crucial roles in the biological functions of proteins, could be  
441 readily characterized by the deuterium-induced isotope shifts on the ε-<sup>13</sup>C signals observed by the  
442 1D <sup>13</sup>C-NMR spectroscopy of a protein selectively labeled with [ε-<sup>13</sup>C; ε,ε-D<sub>2</sub>]-Lys. Both methods  
443 should work equally well for larger proteins, for which previous NMR approaches were rarely

444 applicable. Therefore, these methods will contribute toward clarifying the structural and functional  
445 roles of the Lys residues in biologically important proteins.

446

#### 447 **Acknowledgements:**

448 This work was supported by Grants-in-Aid in Innovative Areas (21121002, 26119005) to M.K.,  
449 and also in part by the Kurata Memorial Hitachi Science and Technology Foundation and by a  
450 Grant-in-Aid for Scientific Research (C) (25440018) to M.T.

451

#### 452 **References:**

453 André, I., Linse, S., and Mulder, F. A.: Residue-specific pKa determination of lysine and  
454 arginine side chains by indirect  $^{15}\text{N}$  and  $^{13}\text{C}$  NMR spectroscopy: application to apo  
455 calmodulin, *J. Am. Chem. Soc.*, 129, 15805-15813. <https://doi.org/10.1021/ja0721824>,  
456 2007.

457 Barbas, C. F. 3rd, Heine, A., Zhong, G., Hoffmann, T., Gramatikova, S., Björnstedt, R., List,  
458 B., Anderson, J., Stura, E. A., Wilson, I. A., and Lerner, R. A.: Immune versus natural  
459 selection: antibody aldolases with enzymic rates but broader scope, *Science*, 278, 2085-  
460 2092. [https://doi: 10.1126/science.278.5346.2085](https://doi:10.1126/science.278.5346.2085), 1997.

461 Cavanagh, J., Fairbrother, W. J., Palmer, A. G., Rance, M., and Skelton, J. J.: *Protein NMR  
462 Spectroscopy: Principles and Practice*, Academic Press, New York, 2007.

463 Chimenti MS, Castañeda CA, Majumdar A, García-Moreno E B. Structural origins of high  
464 apparent dielectric constants experienced by ionizable groups in the hydrophobic core of a  
465 protein. *J. Mol. Biol.*, 405, 361-377, <https://doi:10.1016/j.jmb.2010.10.001>, 2011.

466 Clore, G. M., Bax, A., Driscoll, P. C., Wingfield, P. T., and Gronenborn, A. M.: Assignment of  
467 the side-chain  $^1\text{H}$  and  $^{13}\text{C}$  resonances of interleukin-1 beta using double- and triple-  
468 resonance heteronuclear three-dimensional NMR spectroscopy, *Biochemistry*, 29, 8172-  
469 8184, [https://doi: 10.1021/bi00487a027](https://doi:10.1021/bi00487a027), 1990.

470 Damblon, C., Raquet, X., Lian, L. Y., Lamotte-Brasseur, J., Fonze, E., Charlier, P., Roberts, G.  
471 C., Frère, J. M.: The catalytic mechanism of beta-lactamases: NMR titration of an active-site  
472 lysine residue of the TEM-1 enzyme, *Proc. Natl. Acad. Sci. USA*, 93, 1747-1752,  
473 [https://doi: 10.1073/pnas.93.5.1747](https://doi:10.1073/pnas.93.5.1747), 1996.

474 Dziembowska, T., Hansen, P. E., and Rozwadowski, Z.: Studies based on deuterium isotope  
475 effect on  $^{13}\text{C}$  chemical shifts, *Prog. Nucl. Magn. Reson. Spectrosc.*, 45, 1-29, [https://doi:  
476 10.1016/j.pnmrs.2004.04.001](https://doi:10.1016/j.pnmrs.2004.04.001), 2004.

477 Farmer, B. T. II, and Venters, R. A.: Assignment of aliphatic side-chain  $^1\text{H}/^{15}\text{N}$  resonances in  
478 perdeuterated proteins, *J. Biomol. NMR*, 7, 59-71, [https://doi: 10.1007/BF00190457](https://doi:10.1007/BF00190457). 1996.

479 Fitch, C. A., Karp, D. A., Lee, K. K., Stites, W. E., Lattman, E. E., and García-Moreno, E. B.:  
480 Experimental pK(a) values of buried residues: analysis with continuum methods and role of  
481 water penetration, *Biophys. J.*, 82, 3289-3304, [https://doi: 10.1016/s0006-3495\(02\)75670-1](https://doi:10.1016/s0006-3495(02)75670-1),  
482 2002.

483 Gao, G., Prasad, R., Lodwig, S. N., Unkefer, C. J., Beard, W. A., Wilson, S. H., and London, R.  
484 E.: Determination of lysine pK values using  $[5-^{13}\text{C}]$ lysine: application to the lyase domain of  
485 DNA Pol beta, *J. Am. Chem. Soc.*, 128, 8104-8105, [https://doi: 10.1021/ja061473u](https://doi:10.1021/ja061473u), 2006.

486 García-Moreno, B., Dwyer, J. J., Gittis, A. G., Lattman, E. E., Spencer, D. S., and Stites, W. E.:  
487 Experimental measurement of the effective dielectric in the hydrophobic core of a protein,  
488 *Biophys. Chem.*, 64, 211-224. [https://doi.org/10.1016/S0301-4622\(96\)02238-7](https://doi.org/10.1016/S0301-4622(96)02238-7), 1997.

489 Hansen, P. E.: Isotope effects on nuclear shielding, *Annu. Rep. NMR Spectrosc.*, 15, 105-234,  
490 1983.

491 Harris, T. K., and Turner, G. J.: Structural basis of perturbed pKa values of catalytic groups in  
492 enzyme active sites, *IUBMB Life*, 53, 85-98, [https://doi: 10.1080/15216540211468](https://doi:10.1080/15216540211468), 2002.

493 Highbarger, L. A., Gerlt, J. A., and Kenyon, G. L.: Mechanism of the reaction catalyzed by  
494 acetoacetate decarboxylase. Importance of lysine 116 in determining the pKa of active-site  
495 lysine 115, *Biochemistry*, 35, 41-46. [https://doi: 10.1021/bi9518306](https://doi:10.1021/bi9518306), 1996.

496 Iwahara, J., Jung, Y. S., and Clore, G. M.: Heteronuclear NMR spectroscopy for lysine  $\text{NH}_3$  groups  
497 in proteins: unique effect of water exchange on  $^{15}\text{N}$  transverse relaxation, *J. Am. Chem. Soc.*,  
498 129, 2971-2980. [https://doi: 10.1021/ja0683436](https://doi:10.1021/ja0683436), 2007.

499 Kainosho, M., and Tsuji, T. Assignment of the three methionyl carbonyl carbon resonances in  
500 *Streptomyces subtilisin inhibitor* by a carbon-13 and nitrogen-15 double-labeling technique.  
501 A new strategy for structural studies of proteins in solution, *Biochemistry*, 21, 6273-6279.  
502 [https://doi: 10.1021/bi00267a036](https://doi:10.1021/bi00267a036), 1982.

503 Kainosho, M., Torizawa, T., Iwashita, Y., Terauchi, T., Ono, A. M., and Güntert, P.: Optimal

504 isotope labelling for NMR protein structure determinations, *Nature*, 440, 52–57, [https://doi:](https://doi:10.1038/nature04525)  
505 10.1038/nature04525, 2006.

506 Kesvatera, T., Jönsson, B., Thulin, E., and Linse, S.: Measurement and modelling of sequence-  
507 specific pKa values of lysine residues in Calbindin D9k. *J. Mol. Biol.*, 259, 828-839,  
508 <https://doi.org/10.1006/jmbi.1996.0361>, 1996.

509 Liepinsh, E., Otting, G., and Wüthrich, K.: NMR spectroscopy of hydroxyl protons in aqueous  
510 solutions of peptides and proteins, *J. Biomol. NMR*, 2, 447-465, [https://doi:](https://doi:10.1007/BF02192808)  
511 10.1007/BF02192808, 1992.

512 Liepinsh, E., and Otting, G.: Proton exchange rates from amino acid side chains-implications for  
513 image contrast, *Magn. Reson. Med.*, 35, 30-42, [https://doi: 10.1002/mrm.1910350106](https://doi:10.1002/mrm.1910350106), 1996.

514 Markley, J. L., Bax, A., Arata, Y., Hilbers, C. W., Kaptein, R., Sykes, B. D., Wright, P. E.,  
515 Wüthrich, K.: Recommendations for the presentation of NMR structures of proteins and  
516 nucleic acids, *Eur. J. Biochem.*, 256, 1-15, <https://doi.10.1046/j.1432-1327.1998.2560001.x>,  
517 1998.

518 Markley, J. L., and Kainosho, M.: Stable isotope labeling and resonance assignments in larger  
519 proteins. in *NMR of Macromolecules*, Oxford University Press, 101-152, 1993.

520 Otting, G., and Wüthrich, K.: Studies of protein hydration in aqueous solution by direct NMR  
521 observation of individual protein-bound water molecules, *J. Am. Chem. Soc.*, 111, 1871-1875,  
522 <https://doi.org/10.1021/ja00187a050>, 1989.

523 Otting, G., Liepinsh, E., and Wüthrich, K.: Proton exchange with internal water molecules in the  
524 protein BPTI in aqueous solution, *J. Am. Chem. Soc.*, 113, 4363-4364, [https://](https://doi.org/10.1021/ja00011a068)  
525 [doi.org/10.1021/ja00011a068](https://doi.org/10.1021/ja00011a068), 1991.

526 Poon, D. K., Schubert, M., Au, J., Okon, M., Withers, S. G., and McIntosh, L. P.: Unambiguous  
527 determination of the ionization state of a glycoside hydrolase active site lysine by  $^1\text{H}$ - $^{15}\text{N}$   
528 heteronuclear correlation spectroscopy, *J. Am. Chem. Soc.*, 128, 15388-15389, [https://doi:](https://doi:10.1021/ja065766z)  
529 10.1021/ja065766z, 2006.

530 Segawa T., Kateb F., Duma L., Bodenhausen G., Pelupessy P.: (2008) Exchange rate constants of  
531 invisible protons in proteins determined by NMR spectroscopy. *ChemBioChem*, 9, 537-542,  
532 <https://doi:10.1002/cbic.200700600>, 2008.

533 Stites, W. E., Gittis, A. G., Lattman, E. E., and Shortle, D.: In a staphylococcal nuclease mutant

534 the side-chain of a lysine replacing valine 66 is fully buried in the hydrophobic core, *J. Mol.*  
535 *Biol.*, 221, 7-14, [https://doi: 10.1016/0022-2836\(91\)80195-z](https://doi: 10.1016/0022-2836(91)80195-z), 1991.

536 Takayama, Y., Castañeda, C. A., Chimenti, M., García-Moreno, B., and Iwahara, J.: Direct  
537 evidence for deprotonation of a lysine side chain buried in the hydrophobic core of a protein,  
538 *J. Am. Chem. Soc.*, 130, 6714-6715, <https://doi: 10.1021/ja801731g>, 2008.

539 Takeda, M., Jee, J., Ono, A. M., Terauchi, T., and Kainosho, M.: Hydrogen exchange rate of  
540 tyrosine hydroxyl groups in proteins as studied by the deuterium isotope effect on C $\zeta$  chemical  
541 shifts, *J. Am. Chem. Soc.*, 131, 18556-18562, <https://doi: 10.1021/ja907911y>, 2009.

542 Takeda, M., Jee, J., Terauchi, T., and Kainosho, M.: Detection of the sulfhydryl groups in proteins  
543 with slow hydrogen exchange rates and determination of their proton/deuteron fractionation  
544 factors using the deuterium-induced effects on the <sup>13</sup>C $\beta$  NMR signals, *J. Am. Chem. Soc.*, 132,  
545 6254-6260, <https://doi: 10.1021/ja101205j>, 2010.

546 Takeda, M., Jee, J., Ono, A. M., Terauchi, T., and Kainosho, M.: Hydrogen exchange study on the  
547 hydroxyl groups of Serine and Threonine residues in proteins and structure refinement using  
548 NOE restraints with polar side-chain groups, *J. Am. Chem. Soc.*, 133, 17420-17427,  
549 <https://doi: 10.1021/ja206799v>, 2011.

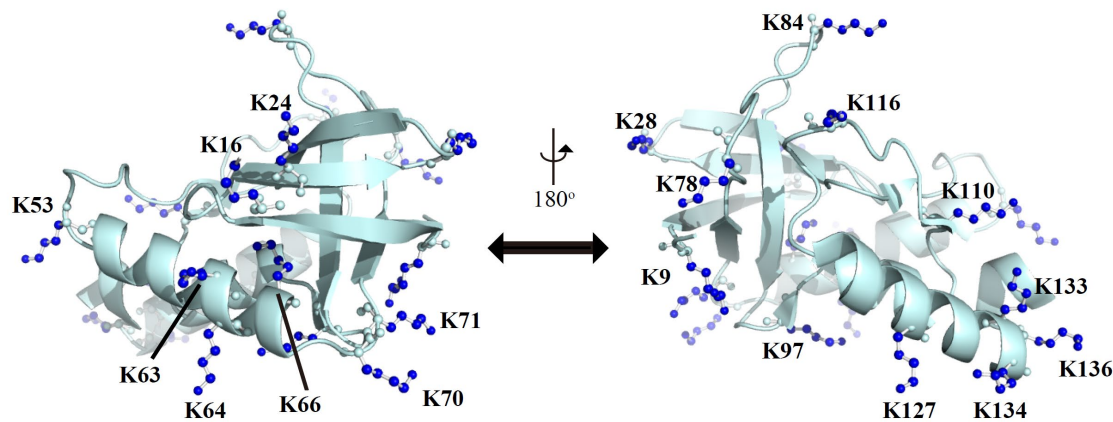
550 Takeda, M., Miyanoiri, Y., Terauchi, T., Yang, C.-J., and Kainosho, M.: Use of H/D isotope effects  
551 to gather information about hydrogen bonding and hydrogen exchange rates, *J. Magn. Reson.*,  
552 241, 148-154, <https://doi: 10.1016/j.jmr.2013.10.001>, 2014.

553 Terauchi, T., Kamikawai, T., Vinogradov, M. G., Starodubtseva, E. V., Takeda, M., and Kainosho,  
554 M.: Synthesis of stereoarray isotope labeled (SAIL) lysine via the "head-to-tail" conversion  
555 of SAIL glutamic acid, *Org. Lett.*, 13, 161-163, <https://doi: 10.1021/ol1026766>, 2011.

556

557  
558

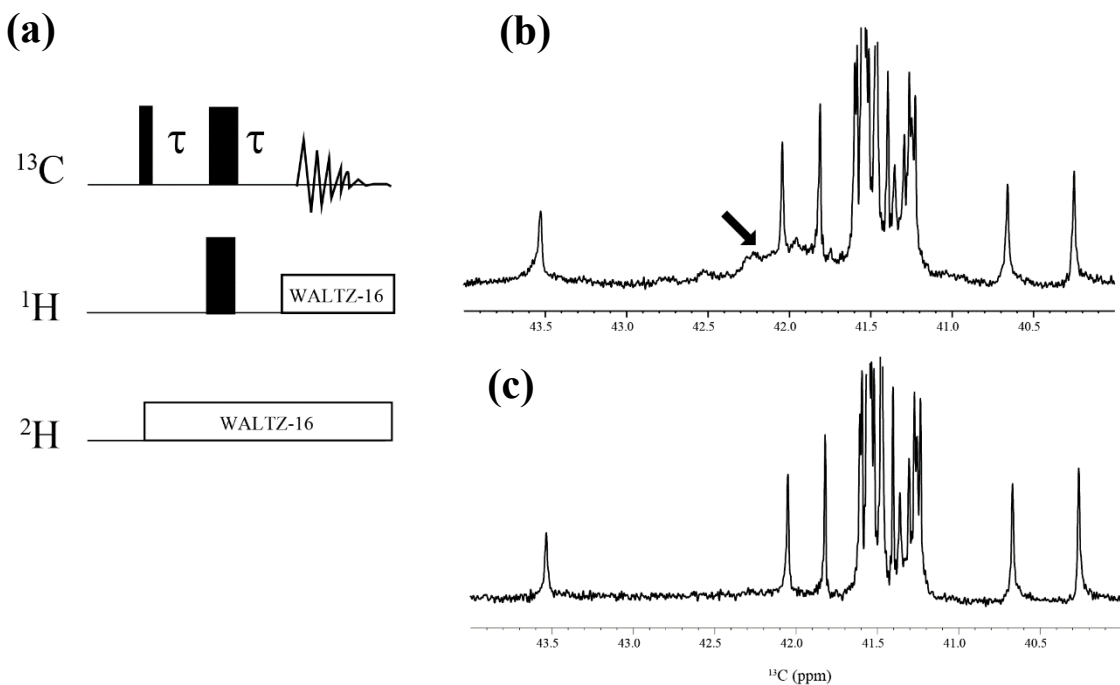
## Appendices



559  
560  
561  
562  
563  
564  
565  
566  
567  
568  
569

**Figure A1: Distribution of the Lys residues in the crystalline structure of the  $\Delta$ +PHS/V66K variant of SNase (PDB#: 3HZX).** All of the side-chain moieties of the Lys residues, which are shown by the ball-and-stick model in blue, exist on the protein surface, except for the Lys-66 (K66). This engineered residue is locked in the protein interior that is originally occupied by the Val sidechain in the wild-type protein. Two Lys residues, K5 and K6, were not visible in the X-ray analysis of the SNase complexed with calcium and thymidine 3',5'-diphosphate and thus it may be slightly different from that in the free state. The figure was created using the Pymol 2.4 software.

570



571

572

573 **Figure A2:  $\{^1\text{H}, ^2\text{D}\}$ -1D  $^{13}\text{C}$  NMR spectra for the SNase variant selectively labeled with  $[\epsilon$ -**

574  $^{13}\text{C};\epsilon,\epsilon\text{-D}_2\text{]-Lys}$ . The 125.7 MHz  $^{13}\text{C}$  NMR spectra were measured at 25 °C on a Bruker Avance 500 spectrometer

575 equipped with a  $^{13}\text{C}$ -observing DCH cryogenic probe. The broad background signals observed in the spectrum (b),

576 indicated by a thick arrow, are due to the natural abundant  $^{13}\text{C}$  atoms bound to proton(s), which are readily filtered out

577 to give the spectrum (c), by using the pulse scheme shown in (a). The narrow and wide bars in the scheme represent

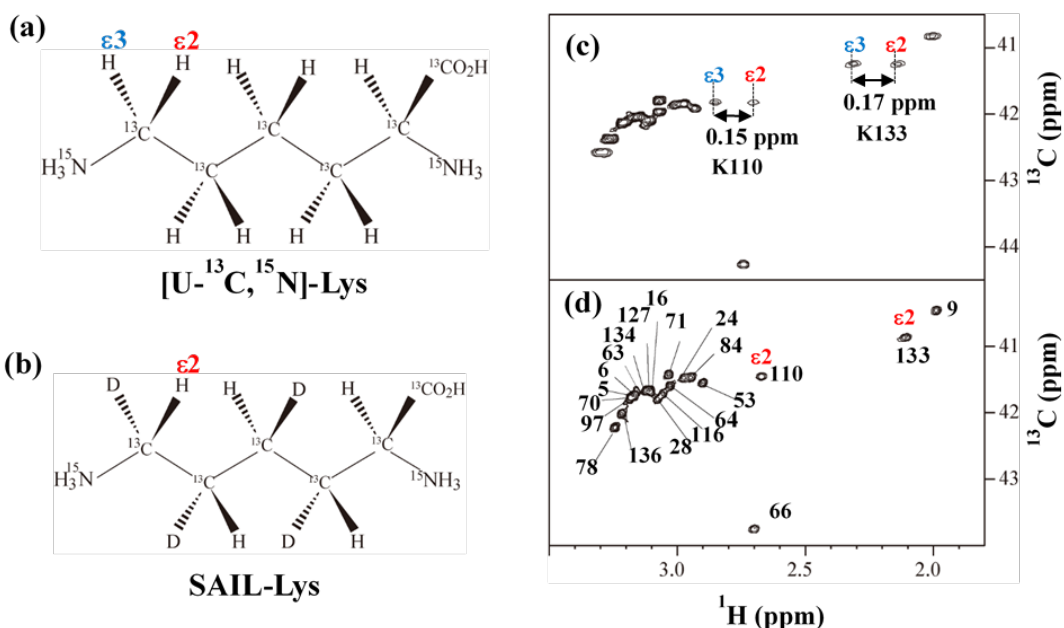
578 90 and 180 ° rectangular pulses, respectively, and are applied along the x-axis at  $\tau = 1.7$  ms, which corresponds to  $1/4$

579  $^1J_{\text{CH}}$ . The SNase variant was dissolved in 100 %  $\text{D}_2\text{O}$  buffer, containing 20 mM sodium phosphate and 100 mM

580 potassium chloride at pH 8.0.

581

582



583

584 **Figure A3: Comparison between the  $^{13}\text{C}^\epsilon$  regions of the 2D  $^1\text{H}$ - $^{13}\text{C}$  constant time (ct-) HSQC**

585 **spectra obtained for the SNase variant selectively labeled with [U- $^{13}\text{C}$ , $^{15}\text{N}$ ]-Lys (a) and [U-**

586  **$^{13}\text{C}$ ,  $^{15}\text{N}$ ; $\beta_2,\gamma_2,\delta_2,\epsilon_3\text{-D}_4$ ]-Lys, SAIL-Lys (b). Since  $\epsilon$ -carbons for the [U- $^{13}\text{C}$ , $^{15}\text{N}$ ]-Lys residues are**

587 **attached to the two prochiral protons,  $^1\text{H}^{\epsilon 2}$  and  $^1\text{H}^{\epsilon 3}$ , a pairwise correlation signals, namely  $^1\text{H}^{\epsilon 2}\text{-}^{13}\text{C}^\epsilon$  and**

588  **$^1\text{H}^{\epsilon 3}\text{-}^{13}\text{C}^\epsilon$ , can be observed for each of the  $\epsilon$ -carbons (c). However, considerable large chemical shift**

589 **difference between the prochiral  $\epsilon$ -methylene protons were observed only for K110 ( $\Delta\delta$ , 0.15 ppm) and for**

590 **K133 ( $\Delta\delta$ , 0.17 ppm), and the other 19 Lys residues showed the differences less than  $\sim 0.05$  ppm. On the**

591 **other hand,  $\epsilon$ -carbons for the SAIL-Lys residues are attached only to the  $\epsilon_2$ -protons, all of the correlation**

592 **signals are automatically assigned to  $^1\text{H}^{\epsilon 2}$  (d).  $\text{C}^\epsilon$  peaks are labeled with their assignment. The spectra were**

593 **measured at 30 °C on an Avance 600 spectrometer equipped with a TXI cryogenic probe.**

594

	$\chi^1$	$\chi^2$	$\chi^3$	$\chi^4$
<b>K5</b>	n.d.	n.d.	n.d.	n.d.
<b>K6</b>	n.d.	n.d.	n.d.	n.d.
<b>K9 Form A</b>	-73	169	-167	-175
<b>Form B</b>	-78	171	-153	44
<b>K16</b>	-171	177	32	-127
<b>K24</b>	-170	157	146	171
<b>K28</b>	-80	177	161	149
<b>K53</b>	-171	164	-164	164
<b>K63</b>	-180	-172	160	73
<b>K64</b>	164	179	174	166
<b>K66</b>	-102	108	81	-73
<b>K70</b>	82	135	171	78
<b>K71</b>	176	164	141	-158
<b>K78</b>	-69	-72	-174	-144
<b>K84</b>	65	-166	166	161
<b>K97</b>	175	176	-155	-144
<b>K110</b>	-83	170	-180	177
<b>K116</b>	-148	134	99	-165
<b>K127</b>	168	66	164	-67
<b>K133</b>	171	156	18	-179
<b>K134</b>	-134	155	-71	126
<b>K136</b>	-68	-112	-143	-50

596

597 **Table A1: List of the dihedral angles ( $\chi^1, \chi^2, \chi^3, \chi^4$ ) in the crystalline state (PDB #3HZX).**